Food Packaging and Shelf Life 55 (2026) 101741

Contents lists available at ScienceDirect

Food Packaging and Shelf Life

journal homepage: www.elsevier.com/locate/fpsl

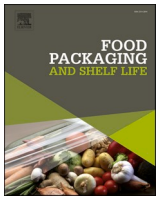

Solvent–free fabrication of pH–sensitive freshness indicators using pomegranate juice in starch–PVA matrix for real–time fish spoilage detection

Evgenia Basdeki [a], Panagiotis Saltouros [a], Enrico Maurizzi [b], Andrea Quartieri [c], Chrysavgi Gardeli [d], Andrea Pulvirenti [b], Theofania Tsironi [a,*]

[a] Laboratory of Food Process Engineering, Department of Food Science and Human Nutrition, Agricultural University of Athens, Iera Odos 75, Athens 11855, Greece
[b] Department of Life Sciences, University of Modena and Reggio Emilia, Modena 41125, Italy
[c] PACKTIN, Via Del Chionso, 14/I, Reggio Emilia 42122, Italy
[d] Laboratory of Food Chemistry and Analysis, Department of Food Science and Human Nutrition, Agricultural University of Athens, Iera Odos 75, Athens 11855, Greece

ARTICLE INFO

Keywords:
Pomegranate juice
Anthocyanins
Starch
Polyvinyl alcohol
Smart packaging
Freshness monitoring

ABSTRACT

Novel freshness indicators were developed using a starch–polyvinyl alcohol matrix incorporating pomegranate juice as a natural source of anthocyanins. To ensure a sustainable production process, the anthocyanins were not isolated from the juice, thus avoiding the use of organic solvents and energy–intensive extraction processes. The resulting smart indicators were characterised in terms of their optical properties, microstructure, infrared spectrum, water affinity, color response across a range of pH values, reactivity to volatile amines (ammonia, trimethylamine and dimethylamine), and color reversibility. The smart indicators were tested in fish fillet packaging systems under controlled temperature conditions (2.8 °C), where their performance was evaluated over time. An artificial intelligence tool was employed to classify the visual appearance of the films during storage. Microstructure analysis revealed satisfactory microstructural integrity and compatibility between the pomegranate juice and the biopolymer carrier. The incorporation of pomegranate juice enhanced the hydrophilicity of the membranes. The color sensitivity test demonstrated that the smart films responded effectively to increases in pH and volatile amine concentrations. A perceptible color shift from red to purple–green was observed from the early stages of spoilage (day 4–5), with intensity increasing as degradation advanced. The indicator response aligned with changes in headspace gas composition and was consistent with microbiological and chemical quality indicators of fish flesh, highlighting their potential as effective tools for real–time monitoring of fish freshness and spoilage.

1. Introduction

In the food industry, packaging is an essential technology for preserving the quality and prolonging the shelf life of fresh but also processed products (Marsh & Bugusu, 2007; Robertson, 2005). Recent interest is focusing on intelligent and smart packaging applications, motivated by the challenge of reducing food waste and limiting food insecurity (Walls et al., 2019; Zhang et al., 2025). At the same time, evolving consumer lifestyles have increased the demand for fresh, hygienic, high quality, and ready–to–eat products with extended shelf life, driving the need for novel food packaging technologies (Shao et al., 2021; Soltani Firouz et al., 2021). This evolution reflects a broader movement away from conventional preservation practices and toward multifunctional packaging systems that can both protect and provide additional information about the product. Within this context, smart packaging has emerged as a valuable alternative to conventional packaging as it integrates sensing or responsive functions into the material itself. More specifically, such materials are designed to track and respond to changes in the micro–environment of the food product, contributing to distinct, non–destructive and real–time monitoring of food quality (D'Almeida & De Albuquerque, 2024; Sohail et al., 2018).

In recent years, it has become clear that traditional packaging materials have raised environmental concerns associated with plastic pollution (Ncube et al., 2020; Yin & Woo, 2024). The food sector utilizes

* Corresponding author.
E-mail address: ftsironi@aua.gr (T. Tsironi).

https://doi.org/10.1016/j.fpsl.2026.101741
Received 19 November 2025; Received in revised form 28 January 2026; Accepted 20 March 2026
Available online 25 March 2026

more than 40% of the packaging materials used globally (Arfelli et al., 2024). Exposure of plastics to stressors such as heat or mechanical force can fragment them into micro– and nanoplastics, which remain in the environment and may eventually circulate back into the food chain (Ali et al., 2024; Athanasopoulou et al., 2025). Bio–based plastics and biopolymers appear as potential sustainable substitutes for petroleum–derived plastic materials due to the environmental burden associated with traditional plastic use (Tsironi & Taoukis, 2018). A major drawback of biobased materials is their typically poor mechanical and barrier properties, which can limit their applicability in food packaging (Helanto et al., 2019). However, studies in recent years have demonstrated that recycled and recyclable packaging options can preserve food while sustaining their shelf life (Basdeki et al., 2023; Tsironi et al., 2022). Beyond reducing the reliance on conventional plastics and promoting the use of biopolymers, the development of more environmentally friendly packaging systems can be further advanced by adopting sustainable production techniques. By this, the limited use of organic solvents and energy consumption as well as the promotion of green extraction methods for active compounds are implied (Janicka et al., 2022; Panja, 2018).

So far, a variety of smart packaging systems have been applied to monitor fish freshness, particularly through the use of pH–sensitive colorants, such as anthocyanins (Pastore et al., 2021; Qin et al., 2021; Sobhan et al., 2022), betalains (Ingale et al., 2025), carotenoids (Ma et al., 2017). Among these, pH–sensitive indicators represent a distinct category of smart packaging technologies, as they offer clear, condition–dependent changes that inform about product freshness in real time without damaging the sample (Jafarzadeh et al., 2024). Several smart packaging systems have focused specifically on anthocyanins extracted from various parts of the pomegranate (*Punica granatum* L.), including fruit juice, seeds, and peels, which are known for their increased levels of bioactive substances, such as phenolic acids, flavonoids, and hydrolysable tannins (Chen et al., 2020). To isolate these compounds, numerous extraction strategies have been reported; from simple ethanol or methanol extraction to combinations of ethanol with acidified water, ethyl acetate fractionation, and Soxhlet techniques (Masci et al., 2016; Abid et al., 2017). Although these methods are effective, they often rely heavily on organic solvents and require high energy input, raising sustainability concerns (Accelerated Solvent Extraction, 2004).

Esfahani et al., (2022) developed smart films based on cassava starch and pomegranate peel powder for monitoring lamb meat freshness and reported a distinct color change in the films changed from purple to green, corresponding to an increase in Total Volatile Basic Nitrogen (TVB–N) levels. Similarly, Ahangari et al., (2025) investigated the development of smart films composed of carboxymethyl cellulose, pomegranate–derived anthocyanins and cellulose acetate nanofibers. In their study, anthocyanins were extracted from pomegranate peels using a water–ethanol solution (70:30 *v*/v). The resulting films effectively monitored spoilage in shrimp and fish, exhibiting significant color changes with ΔE values of 41.74 ± 4.69 and 43.23 ± 4.09, respectively.

In their comparative analysis of pomegranate fractions, Orak et al., (2012) reported that the juice was richer in anthocyanins than the peels and seeds, which also explained its stronger red coloration. So far, no freshness indicators based directly on pomegranate juice, without the use of anthocyanin extraction solvents, have been mentioned in the literature. In this context, the present study aimed to develop pH–sensitive smart films using a starch–polyvinyl alcohol (PVA) matrix and freshly obtained pomegranate juice, extracted solely by direct pressing of the arils, without any prior extraction, concentration, or isolation of anthocyanins. This approach was designed to eliminate the need for organic solvents and energy–intensive procedures, while simultaneously producing an effective and sustainable indicator for monitoring fish freshness.

2. Materials and methods

2.1. Materials

Pomegranate juice was prepared from fresh fruit at the Laboratory of Food Chemistry and Analysis of the Agricultural University of Athens (Athens, Greece). Hydrolyzed starch (molecular weight ≈ 162.14 n g·mol^{-1}) was purchased from Penta Chemicals Unlimited (Prague, Czechia). PVA ($M_n \approx 27$ kDa, 98% degree of hydrolysis) was purchased from Fluka (Steinheim, Germany). Glycerol (≥ 99.5%), citric acid, disodium hydrogen phosphate, and standard aqueous solutions of trimethylamine (TMA), dimethylamine (DMA) and ammonia (NH_3) were purchased from Sigma–Aldrich (St. Louis, MO, USA). Microbiological culture media for microbial enumeration were purchased from Condalab (Torrejon De Ardoz, Spain). Gilthead seabream (*Sparus aurata*) fillets were kindly provided by AVRAMAR SA (Greece).

2.2. Characterization of pomegranate juice

2.2.1. Extraction and identification of anthocyanins content

Pomegranate juice was obtained from fruits of *P. granatum*. L. Cv. Ermioni, and received as described by Gardeli et al., (2019). The extraction of the anthocyanins fraction was carried out using solid–phase extraction (SPE) in C18 cartridges, (500 mg, Macherey–Nagel) as described by Rodriguez-Saona and Wrolstad R.E, (2005), with minor modifications. Chromatographic analysis of the anthocyanins fraction was carried out on a Perkin Elmer Flexar High–performance liquid chromatography (HPLC) (Shelton, CT 06484, USA) system based on the procedure described by Gardeli et al., (2019).

2.2.2. Determination of total monomeric anthocyanin content

Total monomeric anthocyanin content of the juice was measured through spectrophotometry (at 520 and 700 nm) according to the pH differential technique (AOAC Official Method 2005.02). The absorbance difference of the juice measured at pH 1.0 (colored oxonium form) and 4.5 (colorless hemiketal form) at λvis–max 520 nm was proportional to the anthocyanin concentration of the juice. To account for haze, absorbance of the juice was additionally measured at 700 nm. Total monomeric anthocyanin content was calculated using Eq. (1):

Anthocyanin content expressed as cyanidin–3–glucoside (Cy–3–glc) equivalents, mg/L

$$= \frac{A \; x \; MW \; x \; DF \; x1000}{\varepsilon x \; l} \quad (1)$$

Where:

$$A = (Abs_{520\ nm} - Abs_{700\ nm})_{\ pH\ 1.0} - (Abs_{520\ nm} - Abs_{700\ nm})_{\ pH\ 4.5}$$

MW (Molecular weight of the predominant anthocyanin) = 449.2 g/mol for Cy–3–glc,

DF (Dilution factor) = 16 (empirically determined based on the experimental conditions),

ε (Molar absorptivity) = 26,900 L/mol·cm for Cy–3–glc,

l (Path length of the cuvette) = 1 cm.

2.2.3. Optical properties

The color of the pomegranate juice was determined using the i1 PRO color spectrophotometer (X–Rite, Grand Rapids, MI, USA) operated in reflection mode with a D65 light source and 10° observer angle. Measurements were performed by placing the juice in a shallow white ceramic dish to obtain diffuse reflectance from the liquid surface. The color parameters were expressed in the CIE Lab* system, which defines "L" as perceptual lightness, "a" as green to red and "b" as blue to yellow. In addition, light transmittance of the juice was determined using a spectrophotometer (VWR® Douple Beam UV × Vis 6300 PC spectrophotometer, Shanghai, China) in the wavelength range of 380–730 nm

(visible).

2.2.4. pH responsivity

In order to assess the sensitivity of the pomegranate juice to various pH values, pH (2–12) buffer solutions were used following the method described by Qin et al., (2021). The standard buffer solutions consisted of citric acid (0.10 mol·L^{-1}) and disodium hydrogen phosphate (0.20 mol·L^{-1}) aqueous solutions. After exposure to the pH buffer solutions, the color of the juice was measured, and total color difference (ΔE) was calculated based on Eq. (2):

$$\Delta E = \sqrt{(L - L_O)^2 + (a - \alpha_O)^2 + (b - b_O)^2} \quad (2)$$

Where:

L_0, α_0 and b_0: initial color parameters' values,

L, a and b: color parameters' values after pH exposure.

2.3. Preparation of composite films

Smart (PVA/Starch/pomegranate juice) and Control (PVA/Starch) films were prepared using the solution casting method. 2 g PVA per 100 mL (equivalent to 20 g·L^{-1}) and 4 g starch per 100 mL (equivalent to 40 g·L^{-1}) were separately dissolved in deionized water by continuous stirring for 60 min at 90 °C. 10 g glycerol per 100 g of total dry matter was added to the polymer solution as a plasticizer (Qin et al., 2019). After preliminary trials to determine the optimal juice concentration, 15 mL of pomegranate juice was added at 100 mL of total polymer matrix volume. Film–forming solutions (20 mL) were placed into sterilized Petri dishes and dried in the dark for 24 h at 40 °C. The resulting films were stored at 53% relative humidity until further analysis (Basdeki et al., 2025).

2.4. Characterization of composite films

2.4.1. Thickness and optical properties

A digital micrometer (IP65, SAMA Tools, Viareggio, Lucca, Italy) was used to measure the thickness of the composite films at randomly chosen spots. Color parameters and light barrier properties were measured as described in 2.2.3. To determine the transparency of the films, a wavelength of 700 nm was selected, rather than the ASTM standard range of 540–560 nm or the commonly used 600 nm, due to the strong absorbance of anthocyanins near those wavelengths. Since the composite films contained anthocyanins, which exhibit significant absorbance in the visible region, a full–spectrum scan across the visible light range was conducted to distinguish whether the light attenuation was primarily due to chromophore absorption or light scattering (i.e. opacity), as suggested by Zhao et al., (2022). Based on this approach, the opacity of the films was calculated using Eq. (3):

$$\text{Opacity (mm}^{-1}) = -\log(T_{700}) / x \quad (3)$$

Where:

T_{700}: light transmittance at 700 nm,

x: thickness of the films (mm).

2.4.2. Microstructure

Surface (5000x) and cross–section (2000x) micrographs of the composite films were characterized using a scanning electron microscopy (Nova NanoSEM 450, FEI, Hillsboro, OR, USA) equipped with an Everhart–Thornley detector (ETD) operated in high vacuum (HiVac) mode (10^{-2}–10^{-4} Pa) and Field–Free mode at 8 kV.

2.4.3. Fourier transform infrared spectroscopy (FTIR)

Three replicates of each composite film were scanned using an FTIR spectrometer (Alpha, Bruker Optik GmbH, Ettlingen, Germany) with 64 scans (4 cm^{-1} resolution) in the 4000–600 cm^{-1} range.

2.4.4. Moisture content (MC), water solubility (WS) and swelling index (SI)

Five replicates of each composite film (1 cm×5 cm) were tested for water affinity properties such as MC, WS and SI according to the methodology of Romero-Bastida et al. 2005) but with some experimental adjustments described by Basdeki et al., (2025). The equations used to calculate these properties were:

$$MC = \frac{W1 - W2}{W1} x100 \quad (4)$$

$$WS = \frac{W2 - W3}{W2} x100 \quad (5)$$

$$SI = \frac{W4 - W2}{W2} x100 \quad (6)$$

Where:

W_1: initial weight of the films,

W_2: weight of the films after drying (105 °C / 24 h)

W_3: weight of the films after dissolving in water (24 h) and drying (105 °C / 24 h)

W_4: weight of the films after soaking in water (24 h) and soft wiping with tissue paper.

2.4.5. Water sorption isotherms

Water sorption isotherms were used to evaluate the moisture uptake of the composite films under different relative humidity (RH) levels (23, 34, 53, 75, 88, 90, 98%) at two temperatures (5 and 25 °C). The experimental procedure followed was explicitly described by Basdeki et al., (2025). The experimental data were fitted to GAB (Guggenheim–Anderson–de Boer) equation (Blahovec & Yanniotis, 2008):

$$X = \frac{M_O\, C\, a_w}{(1 - a_w)(1 - k\, a_w + C\, k\, a_w)} \quad (7)$$

Where:

X: moisture (g water/g dry basis),

a_w: water activity,

M_0: monolayer moisture of the film on a dry basis,

C: dimensionless parameter accounting for thermal contributions,

k: dimensionless parameter representing the behavior of multilayer water relative to bulk water.

2.4.6. Surface wettability

Surface wettability of the composite films was assessed using a Theta Flow Optical Tensiometer (Biolin Scientific, Gothenburg, Sweden) employing OneAttnesion software, following the ASTM D5946 standard. Fifteen replicates were analyzed of each film type.

2.4.7. pH responsivity of smart indicators

The pH–sensitivity of the composite films was tested across a pH range (2–12), in direct contact with the buffer solutions, based on the method described by Paramera et al., (2011). Color parameters and ΔE of the films were determined as described in 2.2.4.

2.4.8. Sensitivity of smart indicators to volatile amines

TMA, DMA and NH_3 —common microbial metabolites associated with fish spoilage — were individually tested. The smart films were exposed for 1 min to the vapors of aqueous solutions (0.002–1 mol·L^{-1} in distilled water, 25 °C) of each compound to detect visible color change, according to the method described by Kuswandi et al., (2012) with slight modifications described by Basdeki et al., (2025). Since the films were exposed to the gaseous phase above the aqueous solutions, the respective partial pressures of TMA, DMA, and NH_3 at 25 °C were calculated using Henry's law ($p = k_H \cdot C$) at 7.4 – 3.7 10^3 Pa, 3.6 – 1.8 10^3 Pa and 3.3– 1.6 10^3 Pa, respectively. This pressure range is a direct result of the

concentration range used in the aqueous solutions (0.002 – 1 mol L^{-1}). Literature values for Henry constants (Hv) of each volatile substance were used; specifically, Hv ≈ 3.7 Pa·m^3 ·mol^{-1} (TMA), Hv ≈ 1.79 Pa·m^3 ·mol^{-1} (DMA) and Hv ≈ 1.63 Pa·m^3 ·mol^{-1} (NH_3) at 25 °C (Kim et al., 2025; Linstrom, 1997). The calculated partial pressures for the concentration range 0.002–1 mol·L^{-1} are reported in Supplementary Table S1.

2.4.9. Color reversibility of smart indicators

The color reversibility of the films was evaluated by exposing them to the vapors of NH_3 and acetic acid (CH_3COOH), generated from 1 mol·L^{-1} aqueous solutions of each compound (25 °C). Partial pressures of aqueous solutions 1 mol·L^{-1} NH_3 and CH_3COOH at 25 °C were determined at 1.6 10^3 Pa and 14.5 Pa, respectively, as described in 2.4.8. The literature value for Hv of CH_3COOH was 0.0145 Pa·m^3 ·mol^{-1} . Smart films (2 cm×2 cm, 2 replicates) were alternately exposed to the volatile base and acid by placing them 1 cm above 20 mL of each solution, following the method of Yang et al., (2023). After exposure, color parameters and ΔE were calculated according to Eq. (2). The base–acid exposure cycle was repeated until ΔE was minimized, indicating the extent of reversible color change in the films.

2.5. Evaluation of smart indicators in freshness monitoring of fresh fish

2.5.1. Storage of fish under isothermal conditions

To evaluate the effectiveness of the smart films in monitoring fish freshness during storage, a simulation of packaged fish products was developed. Fresh gilthead sea bream (*Sparus aurata*) fillets (50 g) were placed in 15 cm×20 cm sterilized transparent packaging pouches. Packaging was carried out using multilayer blown co-extruded polyethylene/polyamide (PE/PA) pouches with an approximate thickness of 90 μm (oxygen transmission rate <35 cm^3/m^2/24 h at 23°C, 0% RH, ASTM D3985 / ISO 15105–2), supplied by Intrama Protek Ltd., Bulgaria. Two replicates of the smart films (2 cm×2 cm) were pre–attached to the inner surface of each pouch by gentle thermos-sealing, to ensure stable fixation of the indicator film without introducing foreign adhesive materials. The packages were thermo-sealed under atmospheric conditions using the same heat-sealing equipment employed for attaching the indicators and stored at 2.8 °C to simulate typical refrigerated shelf life conditions. The headspace atmosphere corresponded to normal air composition, allowing the evaluation of the indicator's color response exclusively to naturally generated spoilage volatiles without interference from elevated CO_2 levels typical of modified atmosphere packaging.

2.5.2. Determination of microbial growth

The growth of spoilage–related microbial populations in fish fillets (total viable counts–TVC, *Pseudomonas* spp. and Enterobacteriaceae) was monitored daily until complete spoilage. The methodology followed for all microbiological analyses (e.g., sampling, culture media, incubation conditions and final loads enumeration) was performed as described in the studies of Koutsoumanis, (2001) and Tsironi et al., (2019). Two replicates of three appropriate dilutions were enumerated per fish sample and spoilage bacteria.

2.5.3. Determination of spoilage physicochemical markers

pH and TVB–N are key physicochemical indicators of fish spoilage. During the shelf life study, the pH of the fish was measured daily using an edge® HI2002 pH meter (Hanna Instruments Inc., Woonsocket, RI, USA). TVB–N content was determined using Conway's and Byrne's microdiffusion method (Conway & Byrne, 1933).

2.5.4. Determination of in–package gas composition

During the fish shelf life experiment, the in–package gas composition (%O_2, %CO_2) was monitored using a gas analyzer (Danseonsor, CheckPoint 3, Ringsted, Denmark). In–package %N_2 concentration was calculated by difference.

2.5.5. Color change of smart indicators during fish storage

To assess the freshness monitoring efficiency of the smart indicators during fish storage, their color parameters were recorded daily as described in 2.2.3. In brief, the color of the films was measured using the i1 PRO color spectrophotometer (X–Rite, Grand Rapids, MI, USA) operated in reflection mode with a D65 light source and 10° observer angle. Measurements were performed directly on the film surface before use and on the indicators attached inside the packaging during storage, through the transparent pouch. ΔE was also calculated according to Eq. (2).

2.5.6. AI–based discrimination of smart indicators appearance during fish storage

To develop an automated and objective system for monitoring fish spoilage, an AI image classification model was developed using the Azure AI Custom Vision platform (Microsoft) to instantly correlate the visual appearance of the smart indicators with specific spoilage stages. Initially, a dataset of 50 images of smart films (prior to storage) was uploaded to the Custom Vision portal for training an image classification model. The model was trained using Azure's standard algorithm, which automatically optimizes parameters based on the uploaded image content and assigned labels. Model performance was evaluated using built–in platform metrics, including precision, recall, and overall accuracy. Once trained, the model was used to classify test images of smart films, providing predictions along with associated confidence scores. During the fish storage experiment, the smart indicators were photographed daily. The photographs were taken using a Samsung Galaxy A54 set at a fixed distance and under constant, controlled illumination conditions: closed lightbox (Puluz Photo Box, 36 W, 25x25x25 cm) with fixed, diffused illumination (LED 96PCS with a specific color temperature of 5500 K) and including a standardized color reference card (ColorChecker) in every photograph. The resulting images were classified based on their visual appearance using the trained AI model.

2.6. Statistical analysis

Duncan's multiple range test was employed as post–hoc analysis to identify differences of statistical significance (a = 0.05). The Baranyi Growth Model was used for microbial growth data fitting and DMfit 3.5 software (IFR, Institute of Food Research, Reading, UK) was used for curve fitting (available at http://www.combase.cc/index.php/en/, accessed on 14 May 2025).

3. Results and discussion

3.1. Characterization of pomegranate juice

3.1.1. Qualitative determination

The anthocyanin profile of pomegranate juice was characterized by the presence of diglucosides and monoglucosides of delphinidin (Dp), cyanidin (Cy), and pelargonidin (Pg). The results are presented in Table S2. The predominant anthocyanidin was Cy either as monoglucoside or as diglucoside accounting for 28.3% and 24.7% of the total anthocyanins content, respectively. The total concentration of anthocyanins as determined by HPLC after SPE extraction, was found equal to 333.9 ± 0.1 mg·L^{-1} , much higher than the total monomeric anthocyanin content determined by the pH–differential method. Such discrepancies can be attributed to the different solvent system utilized that affects the spectral characteristics of anthocyanins (Lee et al., 2008).

3.1.2. Total monomeric anthocyanin content

Total monomeric anthocyanin content of the juice was 118,63 mg/L Cy–3–glc equivalents. Similar studies have reported total monomeric anthocyanin contents of 72.99 ± 0.27 mg/L (El-Shall et al. 2023) and

102.2 ± 16.4 mg/L (Elfalleh, 2012) Cy–3–glc equivalents using solvent extraction methods with HCl:ethanol (85:15) and methanol, respectively. It is common to expect losses during the solvent extraction processes that are mainly attributed to handling or solvent selectivity. The relatively higher anthocyanin content of the juice is promising for its pH–responsiveness and color–changing capability.

3.1.3. Optical properties

According to the CIE Lab* system, L–value of the pomegranate juice was 28.06 ± 1.99, a–value was 30.59 ± 1.53 and b–value was 8.70 ± 0.65. Light transmittance of the juice dropped from ~4.5% at 420–460 nm to ~1.5% at 480–540 nm, corresponding to the range that anthocyanins absorb, which typically spans 450 – 580 nm, and then increased again to ~18% after 600 nm (Chandra Singh et al., 2022). The pH of the juice during optical properties determination was 3.29 ± 0.18.

3.1.4. pH responsivity

As the pomegranate juice was exposed to varying pH (2–12), the structure of the anthocyanins underwent continuous changes, resulting in corresponding changes in light transmittance and thus visible color, as shown in Fig. 1a, b. The highest light transmittance within the anthocyanins absorption spectrum (450–580 nm) was observed at pH 6, where the juice appeared nearly colorless. In contrast, the lowest transmittance occurred at pH 2, corresponding to an intense red coloration. These observations are consistent with the findings of El-Shall et al. (2023), who reported similar UV–Vis spectral shifts for pomegranate anthocyanins across the same pH 2–12 range. At low pH values (2–3), where anthocyanins present as flavylium cation, a strong red coloration was observed, which was also reflected at the increased a–values. As pH increased (4–7), the color of the juice gradually shifted to colorless or light purple, owing to the formation of carbinol pseudobase and hemiketal structures of anthocyanins. This transition was accompanied by a decline in the a–value from 32 at pH 3–16 at pH 7. Under mildly alkaline conditions (8–11), blue to dark moss–green colorations began to emerge, associated with the formation of anionic quinonoidal base structures. These changes were also evident in the b–values, which increased from 2.6 to 5.4. At pH 12, anthocyanins converted to chalcone form, resulting in a sharp increase in b–value to 16 and a noticeable shift in color to yellow–brown. Throughout the pH sensitivity test, ΔE remained consistently above 3, indicating that the color changes were perceptible to the human eye. ΔE values continued to rise up to pH 12, demonstrating a strong correlation between pH and visible color transformation. The color parameters and ΔE values are presented in Fig. 1c, d.

3.2. Characterization of composite films

3.2.1. Thickness and optical properties

The thickness of a film could influence a range of functional attributes, including its mechanical and optical behavior, morphology, and solubility (Da Silva Filipini et al., 2021). Thickness and optical properties of the composite films are presented in Table 1.

Although no statistically significant differences were observed in thickness, smart films appeared slightly thicker than control ones. This slight difference could be attributed to the incorporation of additional juice components, such as sugars, fibers and other solubles, into the polymer matrix. Visually, the smart films exhibited a reddish–pink hue, as also confirmed by elevated values of the color parameter a. In contrast, the control films were colorless and transparent across the

Table 1
Physicochemical and optical properties of the composite films.

	Smart films	Control films
Thickness (mm)	0.149 ± 0.02^{a}	0.124 ± 0.01^{a}
Opacity (mm^{-1})	2.39 ± 0.02^{a}	1.29 ± 0.11^{b}
L	50.50 ± 0.34^{a}	88.08 ± 1.92^{b}
a	36.55 ± 0.59^{a}	–0.68 ± 0.02^{b}
b	1.68 ± 0.20^{a}	–4.99 ± 0.27^{b}
MC (%)	26.58 ± 2.14^{a}	11.40 ± 0.58^{b}
SI (%)	48.13 ± 3.20^{a}	37.36 ± 3.86^{b}
WS (%)	31.56 ± 4.64^{a}	63.55 ± 6.55^{b}

Values are expressed as mean ± standard deviation. Values with different superscripts in the same row (a, b) were significantly different as shown by Duncan's multiple range test ($p \leq 0.05$).

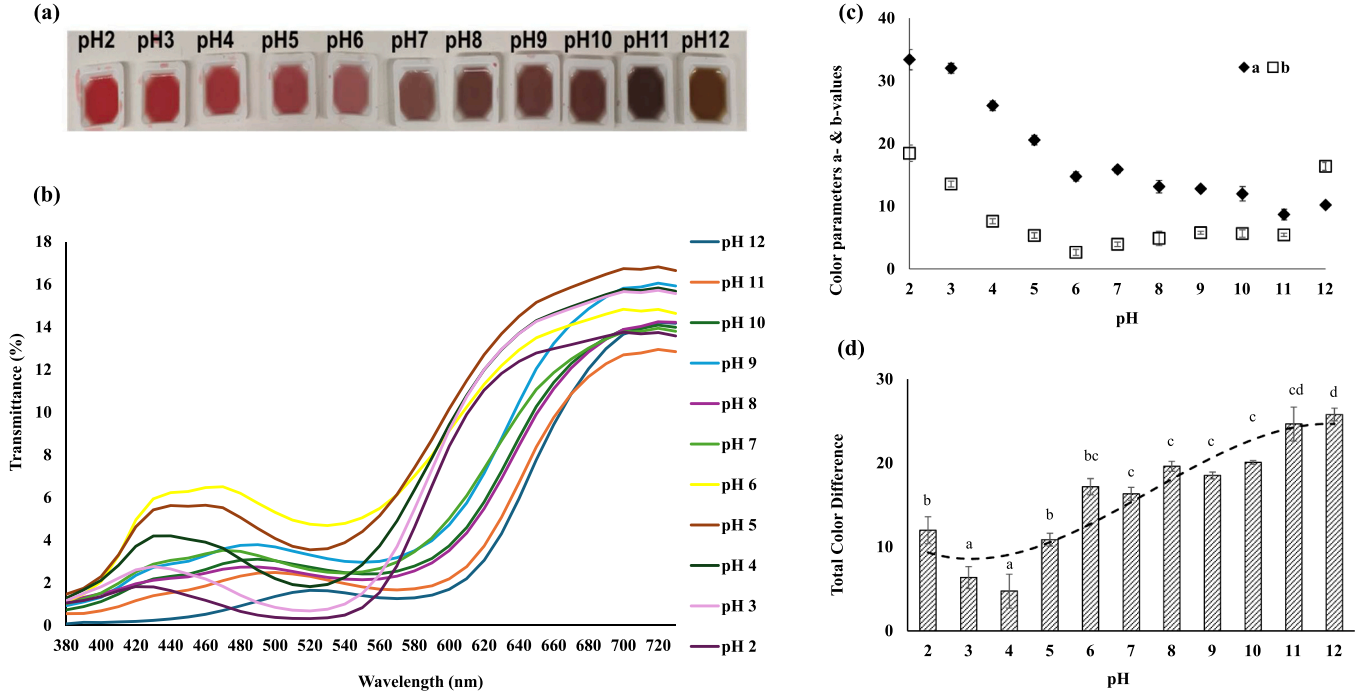

Fig. 1. (a) Digital images, (b) light transmittance (%), (c) color parameters and (d) ΔE of the pomegranate juice after exposure to pH 2–12. Values with different superscripts (a, b, c, d) were significantly different as shown by Duncan's multiple range test ($p \leq 0.05$).

visible light spectrum, as indicated by their low a– and b–values and minimal opacity, a typical characteristic of biopolymer films (Chhikara & Kumar, 2022). The smart films were less transparent than the control films. This reduced transparency could not be solely attributed to the film coloration, since opacity was measured at 700 nm, outside the anthocyanin absorption range, where light scattering, not chromophore absorption, predominates (Zhao et al., 2022). Therefore, the reduced transparency observed in the smart films may be linked to their elevated water content. Several studies have noted that water molecules can promote light scattering inside polymer grids, which in turn contributes to greater opacity (Cazón et al., 2020; Costa et al., 2018; Ren et al., 2017). As depicted in Fig. 2a, the control films demonstrated consistently high light transmittance (approximately 70%) across the entire measured spectrum, indicating excellent optical clarity. In contrast, the smart films exhibited a noticeable drop in light transmittance between 480–540 nm, corresponding to the anthocyanin absorption range. However, this decrease was less pronounced than that observed for the juice alone, suggesting that anthocyanins in the juice were more strongly absorbing than those embedded with the polymer matrix.

Although the films were prepared by solution casting for laboratory feasibility, this approach remains acceptable for small–area indicators (2 cm×2 cm). To bridge the gap toward industrial processing, the use of a film applicator technique could provide better control of thickness and uniformity while serving as a suitable precursor to slot–die or roll–to–roll coating methods employed in large–scale intelligent label production.

3.2.2. *Microstructure*

Characterization of the film morphology provided important information regarding polymer compatibility and the incorporation of pomegranate juice into the polymer matrix. As shown in Fig. 2b(i) and 2b(ii), the control films displayed a compact and uniform surface, reflecting the good compatibility generally observed between PVA and starch. By contrast, the smart films showed noticeable micropores, pointing to alterations in the polymer network associated with the presence of pomegranate juice. Numerous studies have confirmed that PVA and starch blend well, usually producing consistent and well–integrated microstructures (Tian et al., 2017). The lack of any clear phase boundary between the two polymers further implies strong intermolecular interactions (Patil et al., 2021). Although micropores were evenly distributed throughout the smart films—suggesting reasonable miscibility of the system—slight heterogeneity remained at the surface.

To gain additional insights into the inner structure, cross–sectional images were assessed. As illustrated in Fig. 2b(iii) and 2b(iv), the presence of pomegranate juice reduced overall homogeneity and led to signs of phase separation. Importantly, microporous features were also evident in the cross–sectional images of smart films, indicating that the observed heterogeneity is not limited to the surface but extends throughout the bulk of the films. This observation supports the interpretation that the presence of pomegranate juice affects the film formation process rather than resulting from surface preparation or imaging artefacts. Previous studies have reported that polymer matrices or synthesized materials often exhibit more uniform and well-defined morphologies in the absence of plant-derived additives. The incorporation of plant extracts such as rice straw extracts in 3-hydroxybutyrate-co-3-hydroxyvalerate/ polycaprolactone blends (Moll et al., 2025), anthocyanin-rich berry extracts in alginate/carrageenan beads (Salgado et al., 2025), or pomegranate peel in mung bean protein-based active film (Moghadam et al., 2020) has been shown to increase structural heterogeneity, aggregation, and the formation of microporous features, as well as surface defects not observed in control systems.

While these microstructural alterations may be associated with the introduction of low molecular weight constituents present in pomegranate juice, such as sugars or organic acids, alternative mechanisms cannot be excluded (Hulda et al., 2020). Micropore formation may also arise from partial polymer phase separation, or air entrapment during casting and drying (Bui & Choi, 2017; Li et al., 2009). Since no

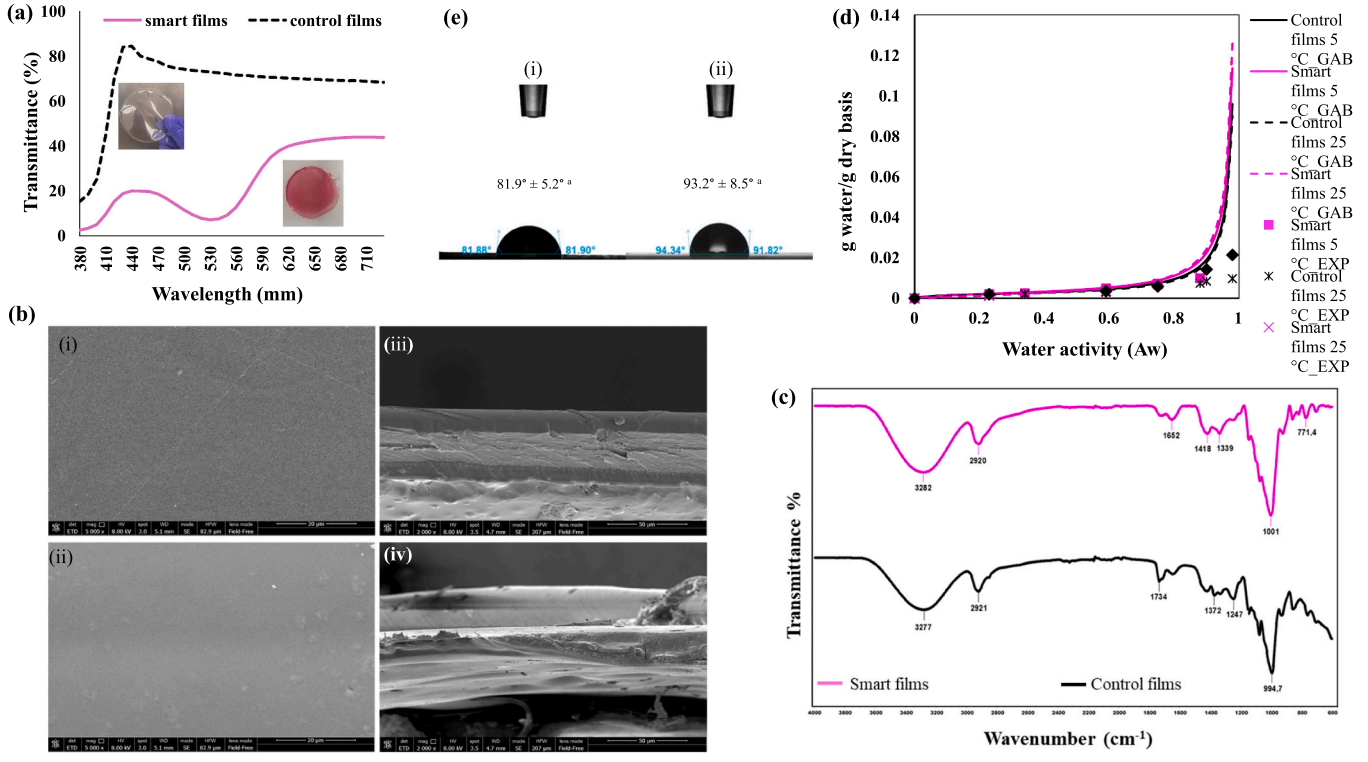

Fig. 2. (a) Light transmittance (%), (b) SEM micrographs of the surface of (i) control and (ii) smart films as well as the cross-sections of (iii) control and (iv) smart films, (c) FT-IR spectra, (d) water sorption isotherms at 5 and 25°C, and (e) WCA (θ°) of composite films. Values with different superscripts (a, b) were significantly different as shown by Duncan's multiple range test ($p \leq 0.05$).

compositional mapping or selective staining was performed, SEM analysis alone cannot confirm the chemical nature of the microporous regions. Accordingly, the potential involvement of juice–derived components is proposed as a plausible hypothesis rather than a definitive mechanism, warranting further investigation using complementary analytical techniques.

3.2.3. Fourier transform infrared spectroscopy

To further assess the incorporation of the pomegranate juice in the polymer structure, FTIR spectra (4000–600 cm^{-1}) were collected for both control and smart films. As shown in Fig. 2c, both control and smart films displayed a broad absorption band at ~3277–3282 cm^{-1}, corresponding to O–H stretching vibrations typical of PVA, consistent with previous reports (Wang et al., 2015). The presence of a C–O stretching peak near 1247 cm^{-1} was also observed and is associated with ether linkages (C–O–C) of starch molecules (Song et al., 2011). The band at 1734 cm^{-1} in the control films was attributed to surface groups of PVA (Kovtun et al., 2024). Upon incorporation of pomegranate juice, noticeable spectral changes were detected, indicating modifications in intermolecular interactions within the polymer matrix. Juice constituents such as polyphenols, anthocyanins, sugars, and organic acids contain abundant hydroxyl and carbonyl groups capable of participating in hydrogen bonding (Krueger, 2012). Accordingly, the shift of the vibration band from 1372 cm^{-1} in the control films to 1339 cm^{-1} in the smart films suggests bond weakening associated with hydrogen bond formation and energy redistribution within the matrix. In addition, a new band at 1418 cm^{-1} appeared in the smart films, which can be related to CH_2 bending vibrations of alkyl groups present in pomegranate-derived polysaccharides (Nordin et al., 2018; Wilpiszewska et al., 2019). Another characteristic signal at 1652 cm^{-1}, was attributed to C═O and C═C stretching, consistent with carbonyl and double-bond functionalities of anthocyanins and other phenolic compounds (Wang & Liu, 2024). Finally, a peak around 771 cm^{-1} was associated with anthocyanins aromatic C—H out–plane bending. Similar absorption bands (925, 879, and 763 cm^{-1}) linked to anthocyanin vibrations have been reported in starch/β–cyclodextrin/carboxymethyl hydrogel systems containing pomegranate peel extract (Savekar et al., 2024).

Overall, FTIR analysis confirms bulk-level chemical interactions between the polymer matrix and pomegranate juice constituents. However, as FTIR does not provide spatially resolved compositional information, these findings cannot directly identify the chemical nature of specific microstructural features observed by SEM.

3.2.4. MC, WS and SI

MC, WS and SI are properties indicative of the functional performance of the composite films and also directly relevant to the practical applicability, scalability, and regulatory compliance of smart packaging materials. The obtained results are presented in Table 1. Smart films were characterized by significantly higher MC compared to control ones, possibly attributed to the presence of juice–derived ingredients, such as sugars and other hydrophilic compounds that absorb and retain moisture (Zhang et al., 2022). This was also reflected in the SI values, indicating that smart films had greater swelling capacity due to the formation of a more open and porous polymeric structure, which was also evident from the FTIR and SEM analysis. These findings suggest that the functional additives introduced in the polymer matrix not only increased the moisture retention ability but also influenced the film's structural response upon exposure to water. Interestingly, although smart films exhibited greater swelling, they were significantly less soluble in water than control films, as reflected in their WS values. In their review on polymer dissolution, Miller-Chou and Koenig, 2003 highlighted that solubility is influenced not only by swelling but also by the structural and morphological characteristics of the polymer, with chain disentanglement—dependent on molecular weight—playing a key role. The lower solubility observed for the smart films may therefore be explained by interactions between pomegranate juice constituents, such as polyphenols, organic acids, and anthocyanins, and the polymer chains. These components are likely to promote hydrogen bonding and physical intermolecular interactions within the matrix, which may act as partial physical crosslinks restricting chain disentanglement and dissolution. This interpretation is consistent with the FTIR results, which revealed peak shifts following the incorporation of pomegranate juice (e.g., 1372 → 1339 cm^{-1}, indicative of energy redistribution associated with hydrogen bond formation) and new absorption bands (C═O at 1652 cm^{-1}) associated with juice-derived functional groups capable of hydrogen bonding (Li et al., 2024; Pereira et al., 2015). These findings, combined with the morphological alterations observed by SEM and the reduced WS despite increased SI, suggest that juice constituents promote physical intermolecular associations acting as partial physical crosslinking points within the matrix, thereby restricting chain disentanglement and dissolution. As a result, the release of soluble material was restricted even though the films absorbed more water. Comparable findings have been described for other smart film systems, where the addition of pH–responsive colorants similarly reduced WS (Ran et al., 2022; Roy & Rhim, 2021).

Despite the reduced WS values exhibited by the smart films compared to the control ones, their solubility (31.56%) exceeded the maximum limit established by EU legislation for materials intended for direct food contact (<10%; Regulations 10/2011 and 450/2009). The materials used in this stud are either food–grade (i.e., starch and pomegranate juice) or recognized as safe for indirect food contact under EU and FDA frameworks (i.e., polyvinyl alcohol). Several practical strategies commonly applied in smart packaging systems could be employed to further reduce WS and facilitate regulatory compliance. These include the introduction of mild physical or chemical crosslinking agents (e.g., citric acid or multivalent ions), surface coating with hydrophobic or semi-permeable layers, and the development of multilayer or laminated structures in which the smart film functions as an indicator layer supported by a water-resistant carrier (Paudel et al., 2025; Saidi et al., 2025). Until such optimization is implemented, the films are best suited for non-contact applications, such as headspace indicator labels protected by a gas-permeable barrier. From a molecular weight perspective, such a configuration is particularly appropriate, as the main constituents of the indicator matrix, including starch and PVA, are high molecular weight polymers (typically $>10^4$–10^5 g/mol) and therefore non-volatile and unable to diffuse through gas-permeable layers. In contrast, spoilage-related volatile compounds released during fish deterioration, such as ammonia (17.03 g/mol), trimethylamine (59.11 g/mol), and other low molecular weight amines, readily permeate these barriers and interact with the indicator. This pronounced difference in molecular weight and volatility further supports the feasibility and safety of the proposed non-contact label design, even in the absence of direct migration testing.

3.2.5. Water sorption isotherms

The intended use of the fabricated freshness indicators is their inclusion inside fish packages to monitor shelf life, where typically RH is higher > 90%; hence, it was essential to determine the effect of varying RH and temperatures on the water sorption behavior of the films. As shown in Fig. 2d, at low water activity, films gained only minor amounts of water. Above $a_w = 0.80$, the uptake rose sharply, giving the typical sigmoidal profile. Fitting and description of the experimental data was conducted by the GAB model (model parameters presented in Table S4) (Blahovec & Yanniotis, 2008). The R^2 coefficients (≥ 0.90) revealed that the GAB model described satisfactorily the sorption of water in all film types. When comparing films of the same type, water sorption of both film types (control and smart) showed no statistically significant differences between 5 and 25 °C. This is in agreement with our previous results regarding long–term storage of control and smart films based on the same polymers (PVA and starch) at 5 and 25 °C, suggesting that water sorption in these cases was affected more by the polymer

molecules than by the addition of anthocyanin extract/juice (Basdeki et al., 2025). In contrast, when comparing films of different types, it was observed that at 5°C there were no statistically significant differences in sorption, while at 25 °C, smart films absorbed a statistically significantly greater amount of water than the control ones. These results point to a temperature–dependent variation in water sorption between control and smart films, indicating that the latter may experience structural modifications at elevated temperatures which increase their ability to absorb water.

Interestingly, smart films at 25 °C that exhibited the highest water sorption exhibited also the lowest C value. The constant C is related to the binding energy of the first layer of water molecules (monolayer) on the surface of the material (Teodoro et al., 2015). An increase in C usually reflects stronger polarity or the presence of additional –OH groups on the surface of the material. The first layer of water binds more strongly to materials with higher C (Roos, 2024). Consequently, smart films may have increased but weaker binding sites – owning higher M_0 but lower C – indicating that they do not bind tightly with water molecules. This behavior may be linked to surface alterations in the smart films following juice incorporation. Such modifications could create binding sites that are more accessible to water but less polar, in contrast to the control films, which exhibited significantly higher C values at both temperatures. In addition, the C parameter declined with rising temperature in both film types, indicating reduced water–binding forces at elevated temperatures, consistent with the observations of Iglesias et al., (2022) on the effect of temperature on the GAB monolayer.

Overall, water sorption results suggested that smart films retain more water, but with weaker bonds; a property that could be beneficial for smart packaging applications since water acts as a medium for dissolving volatile compounds (i.e., amine metabolites) accelerating the chemical reaction with the pH–sensitive dye of the film. The presence of weaker water–binding forces implies that water molecules remain more mobile and reactive, thereby facilitating faster chemical interactions, even with lower concentrations of metabolites. As a result, the diffusion of amines into the film could be enhanced, leading to faster response times and increased sensitivity.

3.2.6. *Surface wettability*

The wettability of the films can be evaluated by the water contact angle (WCA, θ°) of composite films (Lin et al., 2019). WCA pictures are presented in Fig. 2e. Smart films appeared to be less hydrophobic compared to control ones, with average WCA of 81.9° ± 5.2 and 93.2° ± 8.5, respectively. The slightly hydrophilic profile (θ < 90°) with tendency to hydrophobicity exhibited by the smart films could be attributed to the juice–derived ingredients which may have partially functioned as a cross–linking agent and occupied several hydrophilic groups. Moderate hydrophilicity in the polymer grid is a key property of smart packaging materials, as it allows hydrogen and hydroxide ions to diffuse quickly into the polymer grid, supporting efficient ion transport and quick responses of the pH–sensitive dyes (Xiong et al., 2022).

3.2.7. *pH responsivity of smart indicators*

Digital images of the films after pH exposure, along with the corresponding color parameter a– and ΔE values relative to the control films, are depicted in Fig. 3a(i) and 3a(ii). Initially reddish, the films became pale pink at pH 3–4 and shifted to colorless or light purple at pH 5–8. At pH 9–11, a dark moss–green was observed, followed by a lighter green–yellow at pH 12. These changes corresponded with the a–value, which decreased with pH, reaching 0.81 at pH 11, then increasing to 4.45 at pH 12, probably due to chalcone formation. These trends confirm the structural transformations of anthocyanins in response to pH. ΔE of the smart films during the pH–responsivity test remained above 3, indicating that all color changes were perceptible to the human eye. ΔE values continued to increase with pH, reaching a maximum of 35.9 at pH 11, corresponding to the lowest a–value. A slight drop in ΔE was observed within the pH range of 3–4, which can be attributed to the fact that the initial pH of the control film–forming solution was approximately 3.5. Ahangari et al., (2025) examined the pH–responsive

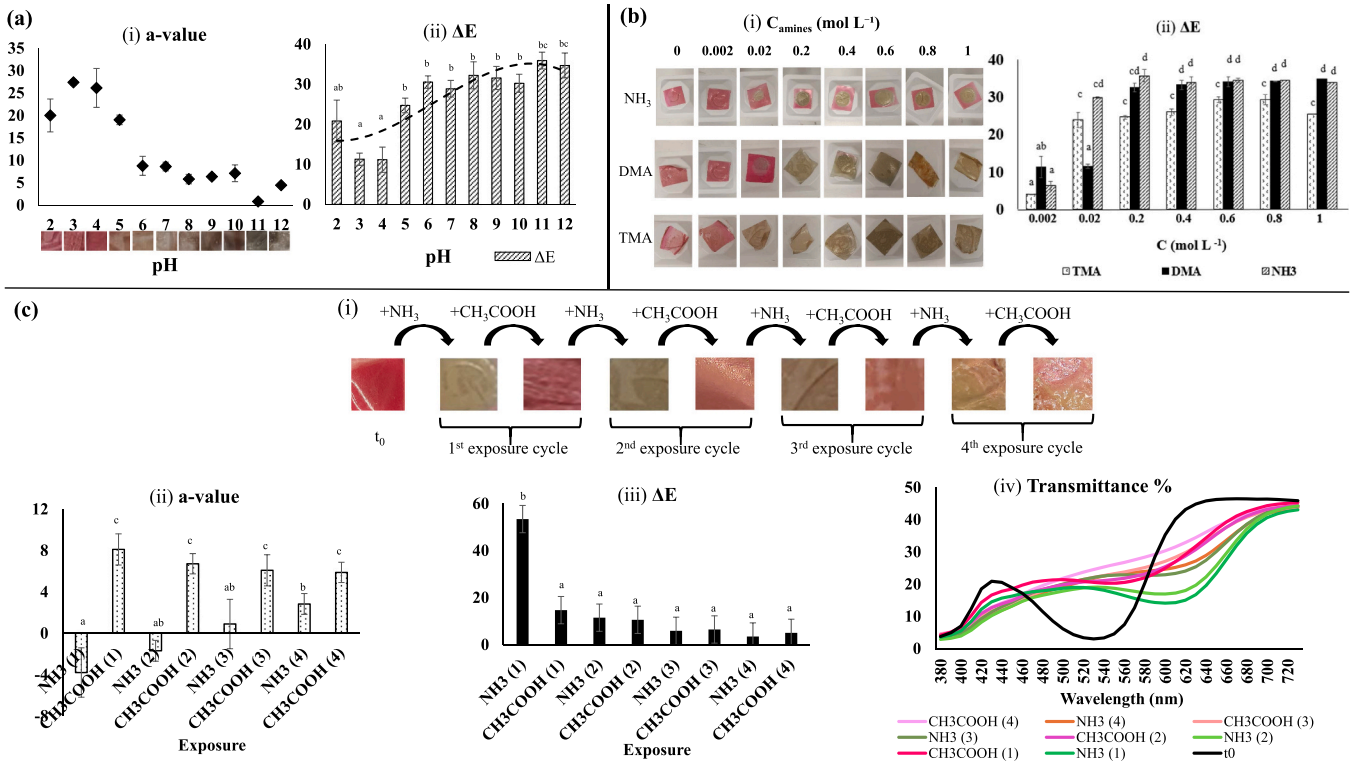

Fig. 3. (a) (i) a-value and (ii) ΔE of the smart films after exposure to pH 2–12, (b) (i) digital images and (ii) ΔE of the smart films after exposure to volatile amines (0.002–1 mol L^{-1}), and (c) Digital images, (ii) a-value, (iii) ΔE and (iv) light transmittance (%) of smart films after repetitive exposure to volatile CH_3COOH (1 mol L^{-1}) and NH_3 (1 mol L^{-1}). Values with different superscripts (a, b, c, d) were significantly different as shown by Duncan's multiple range test ($p \leq 0.05$).

behavior of smart films made from carboxymethyl cellulose, anthocyanins extracted from pomegranate peel, and cellulose acetate nanofibers. They observed lower ΔE values across all pH buffer solutions than those measured in the present study, reporting, for example, ΔE= 3.84 at pH 4, ΔE= 8.48 at pH 7, ΔE= 31.88 at pH 12.

3.2.8. Sensitivity of smart indicators to volatile amines

The degradation of protein tissues by spoilage microorganisms leads to the accumulation of TVB–N compounds, including DMA, TMA, and NH_3, which can alter the pH of the food–film interface (Liu et al., 2018). Fig. 3b(i) and 3b(ii) present the visual color changes and corresponding ΔE values of the smart films following exposure to volatile amines across a concentration range of 0.002–1 mol L^{-1} . Upon exposure to increasing concentrations of NH_3, the films turned from reddish–pink to pale green, particularly within the 0.002 – 0.2 mol L^{-1} range. Beyond a concentration of 0.2 mol L^{-1} , the color of the films exposed to NH_3 shifted to a darker green and remained stable up to 1 mol L^{-1} . This trend was also reflected in the ΔE values, which increased with concentration up to 0.2 mol L^{-1} and then reached a plateau at approximately ΔE= 34. A similar pattern was observed with DMA exposure, i.e. the ΔE values increased steadily up to 0.2 mol L^{-1} and then stabilized around the same ΔE value (ΔE=34). However, the coloration of the films during the DMA test differed slightly from the NH_3 response, appearing more yellowish–golden at 0.8 and 1 mol L^{-1} . This distinction was supported by higher a– and b–values recorded at these concentrations, indicating a stronger chromatic shift toward warm tones. In the case of TMA exposure, the smart films appeared pink at the lowest concentration and progressively shifted to pale green–yellowish in the 0.02–0.4 mol L^{-1} range, followed by a darker green at 0.6 – 1 mol L^{-1} . ΔE values closely followed these visual changes, increasing progressively with concentration. While the films responded to all three volatile amines tested, the highest ΔE values were observed following exposure to NH_3 and DMA, with no statistically significant difference between them above the 0.2 mol L^{-1} concentration. Comparable tests were conducted by Ameri et al., (2024) on smart films containing rice–derived anthocyanins. In their study, the films changed color from red to deep purple/blue and eventually to light brown or dark yellow when exposed to volatile amines.

The broader color palette observed at films after exposure to DMA, ranging from yellow to green hues, may be attributed by the stereochemical structure of DMA compared to TMA. DMA contains only two methyl groups, resulting in lower steric hindrance and a stronger electron–donating effect. This increases the nucleophilicity of the nitrogen atom, making it more reactive an enhancing its interaction with the pH–sensitive compounds in the film (Fernández et al., 2025). In contrast, TMA possesses three methyl groups, leading to greater steric hindrance and higher electron density around the nitrogen. These factors reduce its reactivity and limit its interaction with the film matrix, thereby producing a less pronounced color change (Ghafari et al., 2019; Jen et al., 2014).

3.2.9. Color reversibility of smart indicators

The reversibility of color change is a critical factor in the development of smart freshness indicators (Liu et al., 2019). As demonstrated in Fig. 3c(i) during four consecutive exposure cycles of the smart films to volatile ammonia and acetic acid, a distinct and repeatable color shift was observed from reddish–pink under acidic conditions to green–yellowish under basic conditions. During the initial cycles, the films exhibited higher color reversibility, with rapid and noticeable transitions to reddish and greenish hues upon exposure to CH_3COOH and NH_3, respectively. This reversible behavior was also reflected in the evolution of a–value. As shown at Fig. 3c(ii), the a–value progressively decreased with each NH_3 exposure cycle, although the rate of decrease slowed over time, indicating a declining but still measurable responsiveness. The intensity of the color change decreased progressively with each exposure cycle. Although the color shift remained visible throughout all cycles, ΔE values diminished and eventually reached minimal levels after 4 repetitions. As shown in Fig. 3c(iii), ΔE was approximately 53.4 during the first exposure to NH_3 but dropped significantly to 3.5 by the fourth cycle, indicating a substantial reduction in color responsiveness. Fig. 3c (iv) represents the transmittance spectra of the films before and after repeated exposures to CH_3COOH and NH_3. In the 480–540 nm wavelength range, corresponding to the absorption peak of anthocyanins, transmittance (%) increased notably after the first exposure cycle, indicating loss of chromophore activity and fading of the color intensity. These findings are in line with those of Li et al., (2023), who tested the color reversibility of smart films composed of purple potato anthocyanins, PVA and nanocellulose. Their films maintained sensitivity color changes for up to 3 exposure cycles to CH_3COOH and NH_3, after which color responsiveness declined.

Although the smart films exhibited high initial responsiveness, the substantial decline in ΔE after repeated exposure cycles highlights a limitation in long-term color reversibility. This behavior is likely associated with partial irreversible degradation of anthocyanins under alkaline conditions, including structural rearrangements and loss of chromophore conjugation, as well as possible immobilization or leaching within the hydrophilic polymer matrix (McDougall et al., 2005; Tang et al., 2023). Nevertheless, this limitation does not compromise the intended use of the films as single-use freshness indicators, where a cumulative and non-reversible color response is desirable to reflect spoilage progression. For applications requiring enhanced reversibility, future work could explore anthocyanin stabilization strategies such as encapsulation, co-pigmentation, antioxidant incorporation, or matrix modification through crosslinking or protective coatings.

3.3. Evaluation of smart indicators in freshness monitoring of fresh fish

3.3.1. Microbial growth

Fresh gilthead sea bream fillets were stored under isothermal conditions at 2.8 ± 0.5 °C for nine days (mean value ± standard deviation of the values recorded by the electronic data logger) inside a prototype fish package simulating a bag-type (vertical/sleeve) flow-pack, as shown in Fig. 4a. The growth of the microbial population in the fillets, including the skin, followed a typical sigmoidal trend, in accordance with the time–temperature profile shown in Fig. 4b. Initial TVC were 3.85 ± 0.39 log cfu/g at day 0. The Baranyi model was used to describe microbial growth curves, providing a good fit ($R^2 > 0.9$). During the first four days of storage, TVC increased steadily, with *Pseudomonas spp*. predominating the spoilage microflora, as commonly reported for fish stored under refrigerated, aerobic conditions (Gram & Huss, 1996). Enterobacteriaceae began proliferating after five days of fish storage, though, *Pseudomonas spp.* remained the dominant group throughout the study. Both TVC and *Pseudomonas spp*. showed no lag phase, while Enterobacteriaceae exhibited an approximate two–day lag, likely due to the gradual reduction of oxygen within the packaging, consistent with previous observations Tsironi et al., (2019). Growth kinetic parameters of all spoilage bacteria are presented in Table S3.

3.3.2. Spoilage physicochemical markers

The initial pH of the fish fillets was 6.29 ± 0.07 (day 0). It gradually increased to 6.52 ± 0.08 by day 7, corresponding to the accumulation of volatile amines during fish spoilage. By day 9, the pH slightly decreased to 6.39 ± 0.05, likely due to the production of lactic acid from the fermentation activity of anaerobic bacteria. Throughout storage, TVB–N, which includes TMA, DMA and NH_3, increased steadily. TVB–N levels increased from 7.85 mg/100 g on day 0–18.40 mg/100 g on day 7 and reached 25.24 mg/100 g of fish tissue on day 9, exceeding the commonly accepted spoilage threshold of 25 mg/100 g for fish by the end of the isothermal storage period (Bhadra et al., 2015).

Considering the TVB–N spoilage threshold in combination with the legal limits for acceptable microbial contamination of 7 logcfu/g for TVC (ICMSF, 1986; Papaharisis et al., 2019; Tsironi & Taoukis, 2017),

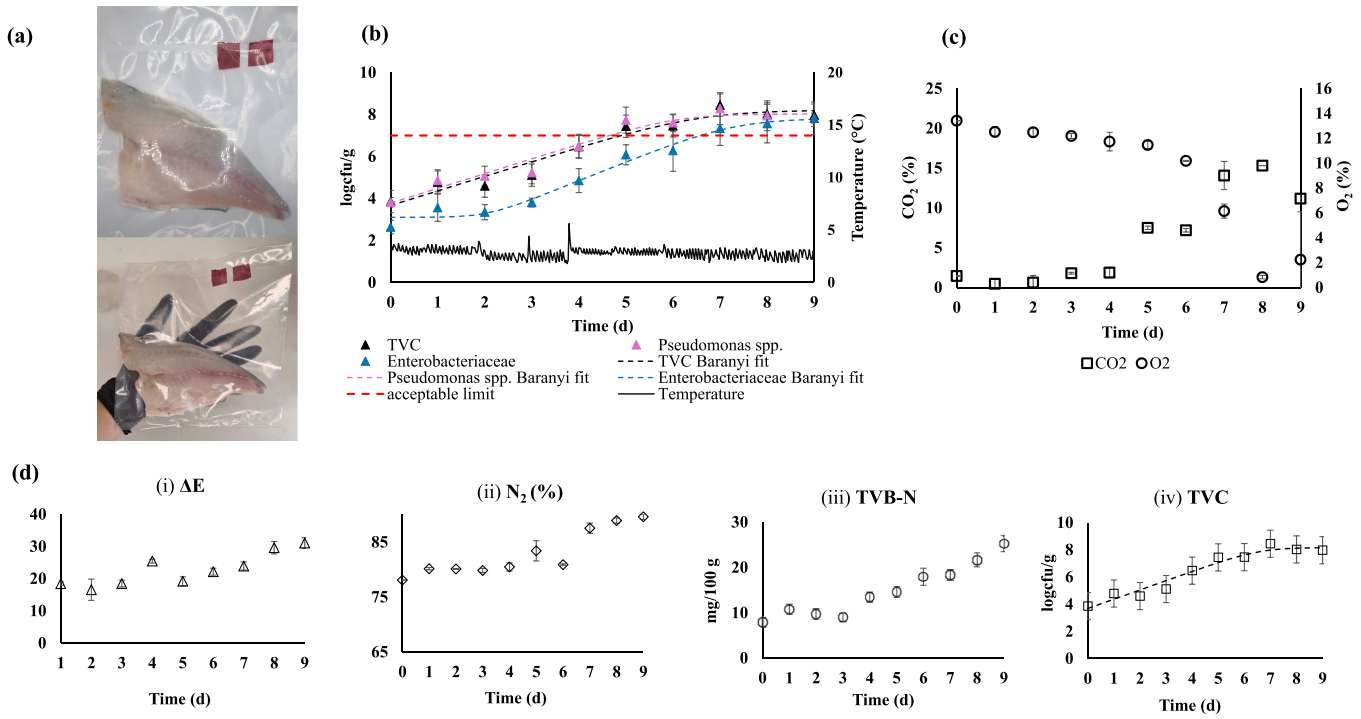

Fig. 4. (a) Prototype of the finished fish package simulating a bag-type (vertical/sleeve) flow-pack, (b) microbial growth of TVC, *Pseudomonas* spp. and Enterobacteriaceae with respect to storage time and temperature, (c) in-package %O_2 and %CO_2, and (d) schematic comparison of (i) ΔE of the smart films, (ii) in-package %N_2, (iii) TVB-N content of fish samples and (iv) microbial growth of TVC during shelf life evaluation of gilthead sea bream fillets at isothermal storage conditions.

the shelf life of sea bream fillets stored at 2.8°C was determined around 6–8 days.

3.3.3. *In–package gas composition*

The headspace gas composition of fish packages is closely correlated with fish freshness throughout storage (Basdeki et al., 2025). At the beginning of the study, fish samples were sealed under atmospheric conditions, consisting of approximately 20.95% O_2, 0.93% CO_2 and 78% N_2. As depicted in Fig. 4c, the O_2 concentration gradually declined to 18.3% by day 4, then dropped more sharply to 9.6% by day 7, reaching 1.3% by day 8. The decrease of in–package oxygen coincided with a limitation in the growth of *Pseudomonas spp.*, which are typically aerobic. Simultaneously, CO_2 levels rose from 1.2% at day 4–9% by day 7, reaching 9.8% on day 8, reflecting aerobic microbial activity in which O_2 is consumed and CO_2 produced (Koutsoumanis et al., 2008). Overall, CO_2 accumulation closely mirrored the increase in TVC, tracking the microbial growth dynamics over time. O_2 depletion occurring at day 8 confirmed the transition from aerobic to anaerobic spoilage conditions, indicating the end of shelf life of sea bream fillets stored at 2.8°C (Zouharová et al., 2023).

3.3.4. *Color change of smart indicators*

The smart indicators presented visible color transformations during the isothermal storage of gilthead sea bream fillets. The corresponding color parameters and digital images of the smart films for each storage day are presented in Table 2. Initially reddish (day 0–1), the films shifted to lighter red–pink (day 2–7) and eventually greenish (day 8–9). Comparable results have been documented in previous studies, such as in Koshy et al., (2024), who prepared smart films composed of biopolymers and anthocyanins extracted from *Clitoria ternatea* flowers, observing similar color changes—from purple to greenish–purple and ultimately green—while monitoring the freshness of sardines. Likewise, Tavassoli et al., (2024) reported a color transition from brownish–yellow to gray in smart indicators containing anthocyanins derived from red poppy, following 72 h of fish storage at 25 °C.

The visual color transformations of the smart films during storage were also clearly reflected in the color parameters. Specifically, a–value consistently decreased during the storage period, signifying a loss of red coloration as spoilage progressed. The a–value dropped sharply from 50.43 ± 0.11 on day 0–30.35 ± 2.76 on day 4 and further to 22.40 ± 1.76 by day 9. These differences were statistically significant ($p \leq 0.05$) suggesting three distinct stages of films coloration, corresponding to different freshness levels of the fish. A similar trend was reported by Kang et al., (2020) who observed a decrease in a–value from 28 to –2 in smart indicators composed of PVA/okra mucilage polysaccharides and rose–derived anthocyanins, during the monitoring of shrimp freshness.

ΔE of the smart films, shown in Fig. 4d(i), rose progressively over the storage period, reaching 25.43 ± 0.62 on day 4 and 31.03 ± 1.68 by day 9. Fig. 4d also provides a comparative schematic illustrating ΔE alongside % N_2, TVB–N, and TVC during the shelf–life assessment of gilthead sea bream fillets under isothermal conditions. The concurrent trends of these parameters indicate a clear relationship between the visual response of the smart films and key microbiological and physicochemical spoilage indicators. The rise in % N_2 corresponds to the accumulation of volatile amine compounds (TVB–N) produced mainly by microbial activity, as reflected by the increasing TVC. The colorimetric response of the smart films can be mechanistically attributed to the diffusion of volatile basic spoilage metabolites from the fish matrix into the package headspace and subsequently into the polymeric indicator layer. As storage progresses, microbial metabolism leads to the formation of volatile amines (e.g., ammonia, trimethylamine) (Abbas et al., 2008). Upon reaching the film, these amines interact with water molecules present in the film matrix, generating ammonium ions (NH_4^+) and hydroxide ions (OH^-), which create an alkaline microenvironment (Huang et al., 2024). The alkaline environment induced by volatile amines triggers structural transitions in anthocyanins: flavylium cation to quinoidal base or anionic form in response to protonation–deprotonation equilibria (Roy & Rhim, 2021). During fish spoilage, the accumulation of volatile amines promotes proton

Table 2
Color parameters and digital images of smart films during isothermal storage of fish samples.

Time (d)	L	a	b	Smart film
0	39.25 ± 0.63^{bcd}	50.43 ± 0.11^{a}	23.29 ± 0.19^{b}	
1	30.43 ± 0.29^{e}	36.35 ± 0.24^{b}	15.34 ± 0.56^{d}	
2	37.30 ± 3.01^{cd}	34.53 ± 1.87^{bc}	27.45 ± 3.30^{a}	
3	34.81 ± 2.36^{d}	32.58 ± 0.99^{bc}	21.78 ± 1.06^{b}	
4	54.72 ± 4.99^{a}	30.35 ± 2.76^{bcd}	15.25 ± 0.62^{d}	
5	39.69 ± 2.43^{bcd}	31.29 ± 1.85^{bcd}	22.18 ± 1.38^{b}	
6	49.51 ± 2.18^{abc}	31.32 ± 1.95^{cd}	18.79 ± 1.09^{c}	
7	40.37 ± 3.52^{bcd}	27.17 ± 1.79^{d}	17.91 ± 1.28^{c}	
8	48.29 ± 5.57^{abc}	22.61 ± 2.15^{e}	18.77 ± 1.94^{c}	
9	51.79 ± 8.10^{ab}	22.40 ± 1.76^{e}	23.33 ± 1.68^{b}	

Values are expressed as mean ± standard deviation. Values with different superscripts in the same column (a, b, c, d, e) were significantly different as shown by Duncan's multiple range test ($p \leq 0.05$).

abstraction (H^+ removal), shifting the equilibrium toward the anionic anthocyanin forms and resulting in a measurable shift of the absorption maximum (λmax), which manifests as a visible color change (from red to blue–green hues). The gradual and monotonic increase in ΔE observed during storage suggests that the diffusion of volatile amines through the headspace and into the starch–PVA matrix is not instantaneous but follows a time-dependent process that mirrors microbial growth and metabolite production. This diffusion-controlled interaction explains the close temporal agreement between the kinetics of TVC, TVB–N, and the color response of the smart films, supporting their suitability for real-time freshness monitoring rather than instantaneous detection (Khogly et al., 2025).

Although the color transition observed in the smart films was not particularly intense, it was still perceptible and consistent with pH–dependent anthocyanin behavior. This moderate visual response can be attributed to the direct use of pomegranate juice, without prior extraction or purification of anthocyanins. Compared to literature-reported anthocyanin-based indicators relying on solvent-extracted pigments, the direct juice incorporation approach eliminates extraction steps that typically increase cost, processing time, and solvent consumption (Sheibani et al., 2024). While purified anthocyanins may offer sharper color contrast or lower detection thresholds, juice-based systems benefit from simplified processing, reduced environmental burden, and lower solvent related costs (Li et al., 2024). Although higher solvent volumes may increase extraction yield, studies have shown that the relationship between solvent volume and yield is not always linear, and excessive solvent use can lead to increased costs and environmental concerns (Guddi & Sarkar, 2024; Yang et al., 2026). In terms of response time, the developed films exhibit a diffusion-controlled color evolution that aligns with microbial spoilage kinetics, comparable to other polymer-based indicators reported in the literature. Furthermore, the response time of the developed smart films upon ammonia exposure falls within the range reported for anthocyanin-based freshness indicators in the literature, including MOF-containing systems responding within minutes (Sun et al., 2025) and electrospun gardenia blue/curcumin films with approximately 1 min detection times (Panwar et al., 2024). The solvent-free fabrication strategy represents a clear environmental advantage, as it avoids the use of organic solvents, additional purification steps, and associated waste streams typically required for anthocyanin extraction (Netravati et al., 2022). Although quantitative life-cycle assessment was beyond the scope of this study, the simplified processing route is expected to result in lower material, energy, and waste footprints, in line with green chemistry principles.

The starch–PVA matrix employed in this study is well established in smart packaging applications; however, the mode of indicator incorporation plays a critical role in defining the resulting matrix properties. In contrast to systems based on solvent-extracted or purified anthocyanins, the direct incorporation of pomegranate juice introduces a complex mixture of low molecular weight compounds, including sugars, organic acids, polyphenols, and minor polysaccharides, which can simultaneously interact with the polymer chains (Mphahlele et al., 2016). Literature reports on films based on extracted or purified anthocyanins frequently describe rapid and pronounced color transitions upon exposure to volatile amines. For example, films incorporating functional carriers, such as defect-engineered UiO-66 combined with anthocyanins, have been reported to exhibit visible color changes within approximately 1 min following ammonia exposure (Lei et al., 2025). This rapid response has been commonly associated in the literature with the high purity of the pigment and the immediate accessibility of the chromophore within the polymer matrix, which facilitate fast acid–base interactions with volatile amines (Hidayaty et al., 2026). By contrast, the more gradual and monotonic color evolution observed in the present juice-based films may reflect a diffusion- and matrix-mediated response, in which volatile amines interact progressively with anthocyanins embedded within a chemically complex (due to the presence of additional juice-derived components) environment (Bao et al., 2026). Overall, these distinctions highlight that the contribution of the present work does not primarily stem from modifications of the polymer matrix itself, but from demonstrating how extraction-free incorporation strategies may influence matrix functionality, sensing dynamics, and application relevance compared to conventional anthocyanin-based smart films.

3.3.5. AI–based discrimination of smart indicators appearance

During the shelf life evaluation of gilthead sea bream fillets under isothermal storage conditions, the smart indicators were photographed daily and their images were classified using an AI tool. The AI model had been previously trained on digital images of the smart films prior to their application in fish freshness monitoring (Day 0). Once images from subsequent storage days (Day 1–Day 9) were provided, the AI tool analyzed and classified each film based on resemblance probability (%) to the Day 0 reference images. The resemblance probability values produced by the model reflected the likelihood that the appearance of each film matched that of the Day 0 films. This probability decreased progressively during storage, from 97% on Day 1–71.2% on Day 5 and 32.9% on Day 9, indicating increasing visual deviation from the original fresh–stage appearance. The AI-based image classification model

demonstrated satisfactory performance, with a precision of 0.77, recall of 0.80, and an average precision (AP) of 0.71. These results indicate a reliable classification of colorimetric responses under controlled conditions, particularly in terms of sensitivity to freshness-related color changes. The relatively high recall is especially relevant for spoilage monitoring applications, where minimizing false-negative classifications is critical. Since all other factors that could affect film appearance (e.g. texture, composition, preparation batch, photography conditions) were controlled, the observed differences were attributed solely to color changes. These changes reflect the fish spoilage status, confirming that the smart indicators responded reliably over time. Overall, the AI model validated that the color change of the smart films was distinct and aligned with the timeline of fish quality deterioration.

4. Study limitations

The present study was conducted under controlled laboratory conditions (constant temperature, absence of light exposure, and a single fish species), which do not fully represent the complexity of real commercial supply chains. In practical distribution and retail environments, fish products are often subjected to temperature fluctuations, intermittent temperature abuse, variable light exposure, and diverse packaging formats, all of which may influence spoilage kinetics, gas accumulation, and indicator response. In addition, different fish species exhibit distinct microbial categories and spoilage pathways, potentially affecting the rate and composition of volatile amine production.

While the strong correlations observed between color change and microbiological and physicochemical spoilage markers validate the sensing concept under controlled conditions, further studies under dynamic temperature regimes, across multiple fish species, and within different packaging systems (e.g., air, vacuum, MAP) are required to fully assess industrial applicability. These aspects represent important directions for future research toward real-world implementation of the proposed smart indicators.

The AI-based image classification implemented in this study was designed as a supportive tool to assist the interpretation of colorimetric changes rather than as a standalone predictive model. The relatively limited size of the training dataset ($n = 50$ images) may constrain model generalization and increase susceptibility to overfitting, despite the application of cross-validation and complementary performance metrics. Classical k-fold cross-validation was not applied, as model training and evaluation were conducted within a cloud-based classification platform. Moreover, image acquisition was performed under controlled lighting and background conditions, which may not fully represent real-world variability encountered in commercial environments. Future studies should therefore focus on expanding the image dataset, incorporating diverse acquisition conditions, and further validating model robustness across different products and packaging formats.

5. Conclusion

Smart indicators were developed by incorporating pomegranate juice into a starch–PVA polymer matrix, without applying any solvent extraction for anthocyanin isolation. Compared to approaches relying on purified or extracted anthocyanins, the direct use of juice offers clear advantages in terms of process simplicity, reduced chemical consumption, and improved sustainability, while minimizing material loss and processing costs reported in extraction-based systems. Although extracted anthocyanins may exhibit higher pigment purity and more intense colorimetric responses, they are often associated with increased processing complexity and potential stability issues arising from solvent exposure and purification steps.

Despite the absence of extraction, the juice retained a high anthocyanin content and the resulting smart films demonstrated sufficient sensitivity to pH changes and volatile amines relevant to fish spoilage. Water affinity analysis indicated low film solubility, suggesting acceptable short-term stability under humid storage conditions. A strong correlation was observed between the color response of the smart indicators and key microbiological and physicochemical spoilage markers in fish, with the kinetics of color change closely mirroring spoilage progression.

In comparison with commercial freshness indicators, which often rely on synthetic dyes or purified pigments and provide qualitative visual responses, such as the ripeSense® (it is originally red and graduates to orange and yellow) (Sharrock & Henzell, 2010) and the OnVu® time-temperature indicator (it changes color from colorless to blue upon UV light irradiation) (Kreyenschmidt et al., 2010), the developed pomegranate-based indicators offer a biodegradable, food-compatible alternative that integrates naturally derived sensing components with digital-assisted interpretation. While the visual color shift of the juice-based films is moderate, coupling the indicator with AI-based image analysis, as demonstrated in this study, enables objective freshness assessment using mobile devices, mitigating limitations related to human perception and lighting variability.

Overall, the findings indicate that the sustainable production strategy based on direct juice incorporation does not compromise functional performance relative to more complex anthocyanin extraction approaches or existing commercial indicators. Future work should address scalability, long-term storage stability, and performance under modified atmosphere packaging (MAP) conditions, including the development of indicators specifically tailored for CO_2 or O_2 leakage detection in packaged fish products.

CRediT authorship contribution statement

Evgenia Basdeki: Writing – original draft, Validation, Methodology, Investigation, Formal analysis, Data curation, Conceptualization. **Panagiotis Saltouros:** Writing – review & editing, Validation, Investigation, Formal analysis. **Enrico Maurizzi:** Writing – review & editing, Validation, Methodology, Investigation, Formal analysis, Data curation. **Andrea Quartieri:** Writing – review & editing, Validation, Supervision, Methodology. **Chrysavgi Gardeli:** Writing – review & editing, Validation, Methodology, Investigation. **Andrea Pulvirenti:** Writing – review & editing, Supervision, Resources, Methodology. **Tsironi Theofania N.:** Writing – review & editing, Validation, Supervision, Resources, Methodology, Investigation, Conceptualization.

Funding

The research work was supported by the Hellenic Foundation for Research and Innovation (HFRI) under the 5th Call for HFRI PhD Fellowships (Fellowship Number: 20599).

This research has received partial funding from the European Union's Horizon 2020 research and innovation programme under the Marie Sklodowska–Curie Grant Agreement no 872217 (ICHTHYS) (https://www.ichthys-eu.org/about).

Declaration of Competing Interest

The authors declare that they have no known competing financial interests or personal relationships that could have appeared to influence the work reported in this paper.

Appendix A. Supporting information

Supplementary data associated with this article can be found in the online version at doi:10.1016/j.fpsl.2026.101741.

Data availability

Data will be made available on request.

References

Abbas, K. A., Mohamed, A., Jamilah, B., & Ebrahimian, M. (2008). A review on correlations between fish freshness and pH during cold storage. *American Journal of Biochemistry and Biotechnology, 4*(4), 416–421. https://doi.org/10.3844/ajbbsp.2008.416.421

Abid, M., Yaich, H., Cheikhrouhou, S., Khemakhem, I., Bouaziz, M., Attia, H., & Ayadi, M. A. (2017). Antioxidant properties and phenolic profile characterization by LC–MS/MS of selected Tunisian pomegranate peels. *Journal of Food Science and Technology, 54*(9), 2890–2901. https://doi.org/10.1007/s13197-017-2727-0

Accelerated Solvent Extraction. (2004). In D. Luthria, D. Vinjamoori, K. Noel, & J. Ezzell, Oil Extraction and Analysis. AOCS Publishing. https://doi.org/10.1201/9781439822340.ch3.

Ahangari, H., Ebrahimi, A., Ehsani, A., & Amjadi, S. (2025). Multipurpose packaging system based on intelligent carboxymethyl cellulose film and activated cellulose acetate electrospun nanofibers for seafoods. *International Journal of Biological Macromolecules, 298*, Article 140115. https://doi.org/10.1016/j.ijbiomac.2025.140115

Ali, S. S., Elsamahy, T., Al-Tohamy, R., & Sun, J. (2024). A critical review of microplastics in aquatic ecosystems: Degradation mechanisms and removing strategies. *Environmental Science and Ecotechnology, 21*, Article 100427. https://doi.org/10.1016/j.ese.2024.100427

Ameri, M., Ajji, A., & Kessler, S. (2024). Characterization of a food-safe colorimetric indicator based on black rice anthocyanin/PET films for visual analysis of fish spoilage. *Packaging Technology and Science, 37*(8), 769–780. https://doi.org/10.1002/pts.2824

Arfelli, F., Roguszewska, M., Torta, G., Iurlo, M., Cespi, D., Ciacci, L., & Passarini, F. (2024). Environmental impacts of food packaging: Is it all a matter of raw materials? *Sustainable Production and Consumption, 49*, 318–328. https://doi.org/10.1016/j.spc.2024.06.032

Athanasopoulou, E., Power, D. M., Flemetakis, E., & Tsironi, T. (2025). Towards the rational use of plastic packaging to reduce microplastic pollution: a mini review. *Journal of Marine Science and Engineering, 13*(7), 1245. https://doi.org/10.3390/jmse13071245

Bao, Y., Cui, H., Si, X., Li, J., Huang, T., & Li, B. (2026). Anthocyanin-based indicator labels for intelligent food packaging: Mechanisms, multiscale regulation, and future perspectives for enhancing color-response performance. *Trends in Food Science & Technology, 168*, Article 105495. https://doi.org/10.1016/j.tifs.2025.105495

Basdeki, E., Maurizzi, E., Bigi, F., Quartieri, A., Pulvirenti, A., & Tsironi, T. (2025). Functionality and storage evaluation of fish freshness indicators based on the incorporation of anthocyanins extracted from winery grape pomace into polyvinyl alcohol/starch films. *Packaging Technology and Science*. https://doi.org/10.1002/pts.70000

Basdeki, E., Mpenetou, E., Papazoglou, P., Ladakis, D., Flemetakis, E., Koutinas, A., & Tsironi, T. (2023). Evaluation of a calcium carbonate-based container for transportation and storage of fresh fish as a sustainable alternative to polystyrene boxes. *Sustainability, 16*(1), 130. https://doi.org/10.3390/su16010130

Basdeki, E., Vasilaki, S. E., Sensi, M., Flemetakis, E., Biscarini, F., Power, D., & Tsironi, T. (2025). Reviewing the correlation of fish quality alteration and in-package headspace composition: Evidence from a pH freshness indicator case study. *International Journal of Food Science, 2025*(1), Article 3576183. https://doi.org/10.1155/ijfo/3576183

Bhadra, S., Narvaez, C., Thomson, D. J., & Bridges, G. E. (2015). Non-destructive detection of fish spoilage using a wireless basic volatile sensor. *Talanta, 134*, 718–723. https://doi.org/10.1016/j.talanta.2014.12.017

Blahovec, J., & Yanniotis, S. (2008). GAB generalized equation for sorption phenomena. *Food and Bioprocess Technology, 1*(1), 82–90. https://doi.org/10.1007/s11947-007-0012-3

Bui, V.-T., & Choi, H.-S. (2017). Surface morphology and wettability control of polymer Substrates: A comparison of water-miscible and water-immiscible mixture solvents. *European Polymer Journal, 93*, 158–166. https://doi.org/10.1016/j.eurpolymj.2017.05.039

Cazón, P., Vázquez, M., & Velázquez, G. (2020). Regenerated cellulose films with chitosan and polyvinyl alcohol: Effect of the moisture content on the barrier, mechanical and optical properties. *Carbohydrate Polymers, 236*, Article 116031. https://doi.org/10.1016/j.carbpol.2020.116031

Chandra Singh, M., Price, W. E., Kelso, C., Charlton, K., & Probst, Y. (2022). Impact of molar absorbance on anthocyanin content of the foods. *Food Chemistry, 386*, Article 132855. https://doi.org/10.1016/j.foodchem.2022.132855

Chen, J., Liao, C., Ouyang, X., Kahramanoğlu, I., Gan, Y., & Li, M. (2020). Antimicrobial activity of pomegranate peel and its applications on food preservation. *Journal of Food Quality, 2020*, 1–8. https://doi.org/10.1155/2020/8850339

Chhikara, S., & Kumar, D. (2022). Edible coating and edible film as food packaging material: A review. *Journal of Packaging Technology and Research, 6*(1), 1–10. https://doi.org/10.1007/s41783-021-00129-w

Conway, E. J., & Byrne, A. (1933). An absorption apparatus for the micro-determination of certain volatile substances: The micro-determination of ammonia. *The Biochemical Journal, 27*(2), 419–429.

Costa, M. J., Marques, A. M., Pastrana, L. M., Teixeira, J. A., Sillankorva, S. M., & Cerqueira, M. A. (2018). Physicochemical properties of alginate-based films: Effect of ionic crosslinking and mannuronic and guluronic acid ratio. *Food Hydrocolloids, 81*, 442–448. https://doi.org/10.1016/j.foodhyd.2018.03.014

Da Silva Filipini, G., Romani, V. P., & Guimarães Martins, V. (2021). Blending collagen, methylcellulose, and whey protein in films as a greener alternative for food packaging: Physicochemical and biodegradable properties. *Packaging Technology and Science, 34*(2), 91–103. https://doi.org/10.1002/pts.2541

D'Almeida, A. P., & De Albuquerque, T. L. (2024). Innovations in Food Packaging: From Bio-Based Materials to Smart Packaging Systems. *Processes, 12*(10), 2085. https://doi.org/10.3390/pr12102085

Elfalleh, W. (2012). Total phenolic contents and antioxidant activities of pomegranate peel, seed, leaf and flower. *Journal of Medicinal Plants Research, 6*(32). https://doi.org/10.5897/JMPR11.995

El-Shall, F. N., Al-Shemy, M. T., & Dawwam, G. E. (2023). Multifunction smart nanocomposite film for food packaging based on carboxymethyl cellulose/Kombucha SCOBY/pomegranate anthocyanin pigment. *International Journal of Biological Macromolecules, 242*, Article 125101. https://doi.org/10.1016/j.ijbiomac.2023.125101

Esfahani, A., Mohammadi Nafchi, A., Baghaei, H., & Nouri, L. (2022). Fabrication and characterization of a smart film based on cassava starch and pomegranate peel powder for monitoring lamb meat freshness. *Food Science & Nutrition, 10*(10), 3293–3301. https://doi.org/10.1002/fsn3.2918

Fernández, J. A. H., Paternina, K. L. O., & Cano-Cuadro, H. (2025). Computational Study of Catalytic Poisoning Mechanisms in Polypropylene Polymerization: The Impact of Dimethylamine and Diethylamine on the Deactivation of Ziegler–Natta Catalysts and Co-Catalysts. *Polymers, 17*(13), 1834. https://doi.org/10.3390/polym17131834

Gardeli, C., Varela, K., Krokida, E., & Mallouchos, A. (2019). Investigation of Anthocyanins Stability from Pomegranate Juice (Punica granatum L. Cv Ermioni) under a Simulated Digestion Process. *Medicines, 6*(3), 90. https://doi.org/10.3390/medicines6030090

Ghafari, M., Cui, Y., Alali, A., & Atkinson, J. D. (2019). Phenol adsorption and desorption with physically and chemically tailored porous polymers: Mechanistic variability associated with hyper-cross-linking and amination. *Journal of Hazardous Materials, 361*, 162–168. https://doi.org/10.1016/j.jhazmat.2018.08.068

Gram, L., & Huss, H. H. (1996). Microbiological spoilage of fish and fish products. *International Journal of Food Microbiology, 33*(1), 121–137. https://doi.org/10.1016/0168-1605(96)01134-8

Guddi, K., & Sarkar, A. (2024). Optimization of green extraction technologies for recovering bioactive compounds from Ixora coccinea waste flower biomass: A comparative response surface methodology and artificial neural network modeling. *Sustainable Chemistry and Pharmacy, 42*, Article 101830. https://doi.org/10.1016/j.scp.2024.101830

Rodriguez-Saona, L. E., & Wrolstad R.E, F.1-Anthocyanins (2005). Handbook of food analytical chemistry, Volume 2: Pigments, Colorants. In R. E. Wrolstad, T. E. Acree, E. A. Decker, M. H. Penner, D. S. Reid, S. J. Schwartz, C. F. Shoemaker, D. Smith, & P. Sporns (Eds.), *Flavors, Texture, and Bioactive Food Components* (pp. 6–69). Hoboken, NJ, USA: John Wiley and sons Inc.

Helanto, K., Matikainen, L., Talja, R., & Rojas, O. J. (2019). Bio-based polymers for sustainable packaging and biobarriers: A critical review. *BioResources, 14*(2), 4902–4951. https://doi.org/10.15376/biores.14.2.helanto

Hidayaty, A. N., Fiddaroini, S., Fahmi, A. L., Maharani, D. L., Fardiyah, Q., Srihardyastutie, A., & Sabarudin, A. (2026). Red amaranth betacyanin–incorporated Cs/PVA colorimetric films as smart sensors for real-time fish freshness monitoring. *Sustainable Chemistry One World, 9*, Article 100190. https://doi.org/10.1016/j.scowo.2026.100190

Huang, K., Wang, L., Deng, Y., Zheng, H., Wu, S., Li, Z., Lei, H., Yu, Q., & Guo, Z. (2024). Development of amine-sensitive intelligent film with MIL-100(Fe) as function filler based on anthocyanins/pectin for monitoring chilled meat freshness. *International Journal of Biological Macromolecules, 270*, Article 132463. https://doi.org/10.1016/j.ijbiomac.2024.132463

Hulda, N. M. C., Bianca, S. D. C., Wiliene, C. D. L., Daniel, C. K., & Flávio, L. S. (2020). Fruit juices in polysaccharides edible films. *African Journal of Food Science, 14*(3), 53–62. https://doi.org/10.5897/AJFS2020.1916

ICMSF. (1986). Sampling Plans for Fish and Shellfish. In MICROORGANISMS IN FOOD 2 Sampling for Microbiological Analysis: Principles and Specific Applications (2nd edn). Blackwell Scientific Publications.

Iglesias, H. A., Baeza, R., & Chirife, J. (2022). A Survey of temperature effects on GAB monolayer in foods and minimum integral entropies of sorption: A review. *Food and Bioprocess Technology, 15*(4), 717–733. https://doi.org/10.1007/s11947-021-02740-w

Ingale, O. S., Bora, P. P., Pawase, P. A., Bashir, O., Shams, R., Patharkar, S. R., & Roy, S. (2025). A review on intelligent packaging systems using betalain-rich biobased composite films in monitoring freshness of fish, shrimp, and meat. *Food and Bioprocess Technology*. https://doi.org/10.1007/s11947-025-03946-y

Jafarzadeh, S., Yildiz, Z., Yildiz, P., Strachowski, P., Forough, M., Esmaeili, Y., Naebe, M., & Abdollahi, M. (2024). Advanced technologies in biodegradable packaging using intelligent sensing to fight food waste. *International Journal of Biological Macromolecules, 261*, Article 129647. https://doi.org/10.1016/j.ijbiomac.2024.129647

Janicka, P., Płotka-Wasylka, J., Jatkowska, N., Chabowska, A., Fares, M. Y., Andruch, V., Kaykhaii, M., & Gębicki, J. (2022). Trends in the new generation of green solvents in extraction processes. *Current Opinion in Greening and Sustainable Chemistry, 37*, Article 100670. https://doi.org/10.1016/j.cogsc.2022.100670

Jen, C. N., McMurry, P. H., & Hanson, D. R. (2014). Stabilization of sulfuric acid dimers by ammonia, methylamine, dimethylamine, and trimethylamine. *Journal of Geophysical Research: Atmospheres, 119*(12), 7502–7514. https://doi.org/10.1002/2014jd021592

Kang, S., Wang, H., Xia, L., Chen, M., Li, L., Cheng, J., Li, X., & Jiang, S. (2020). Colorimetric film based on polyvinyl alcohol/okra mucilage polysaccharide incorporated with rose anthocyanins for shrimp freshness monitoring. *Carbohydrate Polymers, 229*, Article 115402. https://doi.org/10.1016/j.carbpol.2019.115402

Khogly, A. K. M., Hashim, S. B. H., Marappan, G., Shishir, M. R. I., Zhang, K., Mahgoub, B. K. M., Abaker, H. M. A., Zhang, D., Huang, X., Zhihua, L., Zhai, X.,

Tahir, H. E., Zou, X., & Katona, J. (2025). Starch/ polyvinyl alcohol/Brazilein film with enhanced stability by using medium-chain triglycerides emulsion for real-time meat freshness monitoring. *International Journal of Biological Macromolecules, 327*, Article 146989. https://doi.org/10.1016/j.ijbiomac.2025.146989

Kim, S., Chen, J., Cheng, T., Gindulyte, A., He, J., He, S., Li, Q., Shoemaker, B. A., Thiessen, P. A., Yu, B., Zaslavsky, L., Zhang, J., & Bolton, E. E. (2025). PubChem 2025 update. *Nucleic Aci Research, 53*(D1), D1516–D1525. https://doi.org/10.1093/nar/gkae1059

Koshy, R. R., K, V., Reghunadhan, A., Mary, S. K., Koshy, J. T., D, S., Williams, P. G., & Pothan, L. A. (2024). Biofilms from poly-vinyl alcohol/palmyra root sprout with Boswellia serrata, carbon dots and anthocyanin for sensing the freshness of sardine fish. *International Journal of Biological Macromolecules, 273*, Article 132991. https://doi.org/10.1016/j.ijbiomac.2024.132991

Koutsoumanis, K. (2001). Predictive Modeling of the Shelf Life of Fish under Nonisothermal Conditions. *Applied and Environmental Microbiology, 67*(4), 1821–1829. https://doi.org/10.1128/AEM.67.4.1821-1829.2001

Koutsoumanis, K. P., Stamatiou, A. P., Drosinos, E. H., & Nychas, G.-J. E. (2008). Control of spoilage microorganisms in minced pork by a self-developed modified atmosphere induced by the respiratory activity of meat microflora. *Food Microbiology, 25*(7), 915–921. https://doi.org/10.1016/j.fm.2008.05.006

Kovtun, G., Casas, D., & Cuberes, T. (2024). *Influence of Glycerol on the Surface Morphology and Crystallinity of Polyvinyl Alcohol Films*. https://doi.org/10.20944/preprints202406.0744.v1

Kreyenschmidt, J., Christiansen, H., Hübner, A., Raab, V., & Petersen, B. (2010). A novel photochromic time–temperature indicator to support cold chain management. *International Journal of Food Science and Technology, 45*(2), 208–215. https://doi.org/10.1111/j.1365-2621.2009.02123.x

Krueger, D. A. (2012). Composition of pomegranate juice. *Journal of AOAC INTERNATIONAL, 95*(1), 163–168. https://doi.org/10.5740/jaoacint.11-178

Kuswandi, B., Jayus, Restyana, A., Abdullah, A., Heng, L. Y., & Ahmad, M. (2012). A novel colorimetric food package label for fish spoilage based on polyaniline film. *Food Control, 25*(1), 184–189. https://doi.org/10.1016/j.foodcont.2011.10.008

Lee, J., Rennaker, C., & Wrolstad, R. E. (2008). Correlation of two anthocyanin quantification methods: HPLC and spectrophotometric methods. *Food Chemistry, 110*(3), 782–786. https://doi.org/10.1016/j.foodchem.2008.03.010

Lei, J., Li, W., Zhao, Y., Zhang, P., & Gan, Y. (2025). Smart film based on anthocyanin-defective UiO-66 synergistic response for meat freshness monitoring and packaging. *Journal of Food Composition and Analysis, 147*, Article 108092. https://doi.org/10.1016/j.jfca.2025.108092

Li, J.-F., Xu, Z.-L., Yang, H., Yu, L.-Y., & Liu, M. (2009). Effect of TiO2 nanoparticles on the surface morphology and performance of microporous PES membrane. *Applied Surface Science, 255*(9), 4725–4732. https://doi.org/10.1016/j.apsusc.2008.07.139

Li, L., Wang, W., Zheng, M., Sun, J., Chen, Z., Wang, J., & Ma, Q. (2023). Nanocellulose-enhanced smart film for the accurate monitoring of shrimp freshness via anthocyanin-induced color changes. *Carbohydrate Polymers, 301*, Article 120352. https://doi.org/10.1016/j.carbpol.2022.120352

Li, Z., Cui, R., Liu, W., Wang, M., Li, L., Liu, F., Du, B., & Song, L. (2024). Application of green deep eutectic solvents for anthocyanins extraction from grape pomace: Optimization, stability, antioxidant activity, and molecular dynamic simulation. *LWT, 211*, Article 116878. https://doi.org/10.1016/j.lwt.2024.116878

Lin, W., Ni, Y., & Pang, J. (2019). Microfluidic spinning of poly (methyl methacrylate)/konjac glucomannan active food packaging films based on hydrophilic/hydrophobic strategy. *Carbohydrate Polymers, 222*, Article 114986. https://doi.org/10.1016/j.carbpol.2019.114986

Linstrom, P. (1997). *NIST Chemistry WebBook, NIST Standard Reference Database 69 [Data set]*. National Institute of Standards and Technology. https://doi.org/10.18434/T4D303

Liu, J., Wang, H., Guo, M., Li, L., Chen, M., Jiang, Suwei, Li, X., & Jiang, Shaotong (2019). Extract from Lycium ruthenicum Murr. Incorporating κ-carrageenan colorimetric film with a wide pH–sensing range for food freshness monitoring. *Food Hydrocolloids, 94*, 1–10. https://doi.org/10.1016/j.foodhyd.2019.03.008

Liu, J., Wang, H., Wang, P., Guo, M., Jiang, Suwei, Li, X., & Jiang, Shaotong (2018). Films based on κ-carrageenan incorporated with curcumin for freshness monitoring. *Food Hydrocolloids, 83*, 134–142. https://doi.org/10.1016/j.foodhyd.2018.05.012

Ma, Q., Du, L., & Wang, L. (2017). Tara gum/polyvinyl alcohol-based colorimetric NH3 indicator films incorporating curcumin for intelligent packaging. *Sensors and Actuators B: Chemical, 244*, 759–766. https://doi.org/10.1016/j.snb.2017.01.035

Marsh, K., & Bugusu, B. (2007). Food Packaging—Roles, Materials, and Environmental Issues. *Journal of Food Science, 72*(3). https://doi.org/10.1111/j.1750-3841.2007.00301.x

Masci, A., Coccia, A., Lendaro, E., Mosca, L., Paolicelli, P., & Cesa, S. (2016). Evaluation of different extraction methods from pomegranate whole fruit or peels and the antioxidant and antiproliferative activity of the polyphenolic fraction. *Food Chemistry, 202*, 59–69. https://doi.org/10.1016/j.foodchem.2016.01.106

McDougall, G. J., Fyffe, S., Dobson, P., & Stewart, D. (2005). Anthocyanins from red wine – Their stability under simulated gastrointestinal digestion. *Phytochemistry, 66*(21), 2540–2548. https://doi.org/10.1016/j.phytochem.2005.09.003

Miller-Chou, B. A., & Koenig, J. L. (2003). A review of polymer dissolution. *Progress in Polymer Science, 28*(8), 1223–1270. https://doi.org/10.1016/s0079-6700(03)00045-5

Moghadam, M., Salami, M., Mohammadian, M., Khodadadi, M., & Emam-Djomeh, Z. (2020). Development of antioxidant edible films based on mung bean protein enriched with pomegranate peel. *Food Hydrocolloids, 104*, Article 105735. https://doi.org/10.1016/j.foodhyd.2020.105735

Moll, E., Ferri, A., & Chiralt, A. (2025). PHBV/PCL blend films with active compounds to prolong the shelf life of meat. *Food Packaging and Shelf Life, 52*, Article 101677. https://doi.org/10.1016/j.fpsl.2025.101677

Mphahlele, R. R., Fawole, O. A., Mokwena, L. M., & Opara, U. L. (2016). Effect of extraction method on chemical, volatile composition and antioxidant properties of pomegranate juice. *South African Journal of Botany, 103*, 135–144. https://doi.org/10.1016/j.sajb.2015.09.015

Ncube, L. K., Ude, A. U., Ogunmuyiwa, E. N., Zulkifli, R., & Beas, I. N. (2020). Environmental Impact of Food Packaging Materials: A Review of Contemporary Development from Conventional Plastics to Polylactic Acid Based Materials. *Materials, 13*(21), 4994. https://doi.org/10.3390/ma13214994

Netravati, Gomez, Pathrose, S., N, B., M. R, P., J, M., & Kuruvila, B. (2022). Comparative evaluation of anthocyanin pigment yield and its attributes from Butterfly pea (Clitorea ternatea L.) flowers as prospective food colorant using different extraction methods. *Future Foods, 6*, Article 100199. https://doi.org/10.1016/j.fufo.2022.100199

Nordin, N. A., Rahman, N. A., Talip, N., & Yacob, N. (2018). Citric Acid Cross-Linking of Carboxymethyl Sago Starch Based Hydrogel for Controlled Release Application. *Macromolecular Symposia, 382*(1), Article 1800086. https://doi.org/10.1002/masy.201800086

Orak, H. H., Yagar, H., & Isbilir, S. S. (2012). Comparison of antioxidant activities of juice, peel, and seed of pomegranate (Punica granatum L.) and inter-relationships with total phenolic, Tannin, anthocyanin, and flavonoid contents. *Food Science and Biotechnology, 21*(2), 373–387. https://doi.org/10.1007/s10068-012-0049-6

Panja, P. (2018). Green extraction methods of food polyphenols from vegetable materials. *Current Opinion in Food Science, 23*, 173–182. https://doi.org/10.1016/j.cofs.2017.11.012

Panwar, A., Kumar, S., Dhiman, A., Kumar, V., Gupta, D., & Sharma, A. (2024). pH sensitive indicator film based intelligent packaging systems of perishables: Developments and challenges of last decade. *Microchemical Journal, 207*, Article 111732. https://doi.org/10.1016/j.microc.2024.111732

Papaharisis, L., Tsironi, T., Dimitroglou, A., Taoukis, P., & Pavlidis, M. (2019). Stress assessment, quality indicators and shelf life of three aquaculture important marine fish, in relation to harvest practices, water temperature and slaughter method. *Aquaculture Research, 50*(9), 2608–2620. https://doi.org/10.1111/are.14217

Paramera, E. I., Konteles, S. J., & Karathanos, V. T. (2011). Stability and release properties of curcumin encapsulated in Saccharomyces cerevisiae, β-cyclodextrin and modified starch. *Food Chemistry, 125*(3), 913–922. https://doi.org/10.1016/j.foodchem.2010.09.071

Pastore, A., Badocco, D., Bogialli, S., Cappellin, L., & Pastore, P. (2021). Behavior of Sulfonephthalein and Azo dyes as effective pH sensors in hybrid materials. *Microchemical Journal, 160*, Article 105605. https://doi.org/10.1016/j.microc.2020.105605

Patil, S., Bharimalla, A. K., Mahapatra, A., Dhakane-Lad, J., Arputharaj, A., Kumar, M., Raja, A. S. M., & Kambli, N. (2021). Effect of polymer blending on mechanical and barrier properties of starch-polyvinyl alcohol based biodegradable composite films. *Food Bioscience, 44*, Article 101352. https://doi.org/10.1016/j.fbio.2021.101352

Paudel, S., Regmi, S., Bhattarai, S., Fennell, A., & Janaswamy, S. (2025). Valorization of grapevine agricultural waste into transparent and high-strength biodegradable films for sustainable packaging. *Sustainable Food Technology, 3*(4), 1218–1231. https://doi.org/10.1039/D5FB00211G

Pereira, V. A., De Arruda, I. N. Q., & Stefani, R. (2015). Active chitosan/PVA films with anthocyanins from Brassica oleraceae (Red Cabbage) as Time–Temperature Indicators for application in intelligent food packaging. *Food Hydrocolloids, 43*, 180–188. https://doi.org/10.1016/j.foodhyd.2014.05.014

Qin, Y., Liu, Y., Yong, H., Liu, Jing, Zhang, X., & Liu, Jun (2019). Preparation and characterization of active and intelligent packaging films based on cassava starch and anthocyanins from Lycium ruthenicum Murr. *International Journal of Biological Macromolecules, 134*, 80–90. https://doi.org/10.1016/j.ijbiomac.2019.05.029

Qin, Y., Yun, D., Xu, F., Chen, D., Kan, J., & Liu, J. (2021). Smart packaging films based on starch/polyvinyl alcohol and Lycium ruthenicum anthocyanins-loaded nanocomplexes: Functionality, stability and application. *Food Hydrocolloids, 119*, Article 106850. https://doi.org/10.1016/j.foodhyd.2021.106850

Ran, R., Chen, S., Su, Y., Wang, L., He, S., He, B., Li, C., Wang, C., & Liu, Y. (2022). Preparation of pH-colorimetric films based on soy protein isolate/ZnO nanoparticles and grape-skin red for monitoring pork freshness. *Food Control, 137*, Article 108958. https://doi.org/10.1016/j.foodcont.2022.108958

Ren, L., Yan, X., Zhou, J., Tong, J., & Su, X. (2017). Influence of chitosan concentration on mechanical and barrier properties of corn starch/chitosan films. *International Journal of Biological Macromolecules, 105*, 1636–1643. https://doi.org/10.1016/j.ijbiomac.2017.02.008

Robertson, G. L. (2005). *Food Packaging: Principles and Practice, Second Edition (0 edn.* CRC Press. https://doi.org/10.1201/9781420056150

Romero-Bastida, C. A., Bello-Pérez, L. A., García, M. A., Martino, M. N., Solorza-Feria, J., & Zaritzky, N. E. (2005). Physicochemical and microstructural characterization of films prepared by thermal and cold gelatinization from non-conventional sources of starches. *Carbohydrate Polymers, 60*(2), 235–244. https://doi.org/10.1016/j.carbpol.2005.01.004

Roos, Y. H. (2024). Water sorption modeling and monolayer of biological and food materials. *LWT, 201*, Article 116271. https://doi.org/10.1016/j.lwt.2024.116271

Roy, S., & Rhim, J.-W. (2021). Anthocyanin food colorant and its application in pH-responsive color change indicator films. *Critical Reviews in Food Science and Nutrition, 61*(14), 2297–2325. https://doi.org/10.1080/10408398.2020.1776211

Saidi, L., Wang, Y., Wich, P. R., & Selomulya, C. (2025). Polysaccharide-based edible films—Strategies to minimize water vapor permeability. *Current Opinion in Food Science, 61*, Article 101258. https://doi.org/10.1016/j.cofs.2024.101258

Salgado, F., Sbarbaro, C., Leal, M., Galdames, F., Díaz-Franulic, I., Cantero, P., Durango, D., Forero-Doria, O., Vázquez, P., Dueñas, F., & Duarte, Y. (2025). Physicochemical properties and gastrointestinal release of Chilean endemic berry extracts via biopolymer encapsulation. *LWT, 237*, Article 118693. https://doi.org/10.1016/j.lwt.2025.118693

Savekar, P. L., Nadaf, S. J., Killedar, S. G., Kumbar, V. M., Hoskeri, J. H., Bhagwat, D. A., & Gurav, S. S. (2024). Citric acid cross-linked pomegranate peel extract-loaded pH-responsive β-cyclodextrin/carboxymethyl tapioca starch hydrogel film for diabetic wound healing. *International Journal of Biological Macromolecules, 274*, Article 133366. https://doi.org/10.1016/j.ijbiomac.2024.133366

Shao, P., Liu, L., Yu, J., Lin, Y., Gao, H., Chen, H., & Sun, P. (2021). An overview of intelligent freshness indicator packaging for food quality and safety monitoring. *Trends in Food Science & Technology, 118*, 285–296. https://doi.org/10.1016/j.tifs.2021.10.012

Sharrock, K. R., & Henzell, R. F. (2010). Ethylene ripening of pears by unconventional means: Use of experimental thimble-sized ethylene capsules inside cartons and clamshells. *Acta Horticulturae, 880*, 339–346. https://doi.org/10.17660/ActaHortic.2010.880.40

Sheibani, S., Jafarzadeh, S., Qazanfarzadeh, Z., Osadee Wijekoon, M. M. J., Mohd Rozalli, N. H., & Mohammadi Nafchi, A. (2024). Sustainable strategies for using natural extracts in smart food packaging. *International Journal of Biological Macromolecules, 267*, Article 131537. https://doi.org/10.1016/j.ijbiomac.2024.131537

Sobhan, A., Muthukumarappan, K., & Wei, L. (2022). A biopolymer-based pH indicator film for visually monitoring beef and fish spoilage. *Food Bioscience, 46*, Article 101523. https://doi.org/10.1016/j.fbio.2021.101523

Sohail, M., Sun, D.-W., & Zhu, Z. (2018). Recent developments in intelligent packaging for enhancing food quality and safety. *Critical Reviews in Food Science and Nutrition, 58*(15), 2650–2662. https://doi.org/10.1080/10408398.2018.1449731

Soltani Firouz, M., Mohi-Alden, K., & Omid, M. (2021). A critical review on intelligent and active packaging in the food industry: Research and development. *Food Research International, 141*, Article 110113. https://doi.org/10.1016/j.foodres.2021.110113

Song, D., Thio, Y. S., & Deng, Y. (2011). Starch nanoparticle formation via reactive extrusion and related mechanism study. *Carbohydrate Polymers, 85*(1), 208–214. https://doi.org/10.1016/j.carbpol.2011.02.016

Sun, W., Huo, Y., Feng, X., Wei, L., Lu, X., Liu, S., & Gao, Z. (2025). Recent advances in metal-organic frameworks (MOFs)-based colorimetric sensors for visual detection of food freshness. *Coordination Chemistry Reviews, 535*, Article 216638. https://doi.org/10.1016/j.ccr.2025.216638

Tang, R., He, Y., & Fan, K. (2023). Recent advances in stability improvement of anthocyanins by efficient methods and its application in food intelligent packaging: A review. *Food Bioscience, 56*, Article 103164. https://doi.org/10.1016/j.fbio.2023.103164

Tavassoli, M., Khezerlou, A., Bakhshizadeh, M., Ebrahimi, A., Abedi-Firoozjah, R., Alizadeh-Sani, M., Mohammadian, E., Ehsani, A., & Hashemi, M. (2024). Smart packaging containing red poppy anthocyanins for fish freshness monitoring. *Journal of Food Measurement and Characterization, 18*(4), 3054–3068. https://doi.org/10.1007/s11694-024-02386-0

Teodoro, A. P., Mali, S., Romero, N., & De Carvalho, G. M. (2015). Cassava starch films containing acetylated starch nanoparticles as reinforcement: Physical and mechanical characterization. *Carbohydrate Polymers, 126*, 9–16. https://doi.org/10.1016/j.carbpol.2015.03.021

Tian, H., Yan, J., Rajulu, A. V., Xiang, A., & Luo, X. (2017). Fabrication and properties of polyvinyl alcohol/starch blend films: Effect of composition and humidity. *International Journal of Biological Macromolecules, 96*, 518–523. https://doi.org/10.1016/j.ijbiomac.2016.12.067

Tsironi, T. N., Chatzidakis, S. M., & Stoforos, N. G. (2022). The future of polyethylene terephthalate bottles: Challenges and sustainability. *Packaging Technology and Science, 35*(4), 317–325. https://doi.org/10.1002/pts.2632

Tsironi, T. N., & Taoukis, P. S. (2017). Effect of storage temperature and osmotic pre-treatment with alternative solutes on the shelf-life of gilthead seabream (Sparus aurata) fillets. *Aquaculture and Fisheries, 2*(1), 39–47. https://doi.org/10.1016/j.aaf.2016.10.003

Tsironi, T. N., & Taoukis, P. S. (2018). Current practice and innovations in fish packaging. *Journal of Aquatic Food Product Technology, 27*(10), 1024–1047. https://doi.org/10.1080/10498850.2018.1532479

Tsironi, T., Ntzimani, A., Gogou, E., Tsevdou, M., Semenoglou, I., Dermesonlouoglou, E., & Taoukis, P. (2019). Modeling the effect of active modified atmosphere packaging on the microbial stability and shelf life of gutted sea bass. *Applied Sciences, 9*(23), 5019. https://doi.org/10.3390/app9235019

Walls, H., Baker, P., Chirwa, E., & Hawkins, B. (2019). Food security, food safety & healthy nutrition: Are they compatible? *Global Food Security, 21*, 69–71. https://doi.org/10.1016/j.gfs.2019.05.005

Wang, C., & Liu, C. (2024). A pH-Sensitive Intelligent Packaging Film Harnessing Anthocyanin for Food Freshness Monitoring. *Food and Bioprocess Technology, 17*(12), 5312–5323. https://doi.org/10.1007/s11947-024-03431-y

Wang, T., Li, Y., Geng, S., Zhou, C., Jia, X., Yang, F., Zhang, L., Ren, X., & Yang, H. (2015). Preparation of flexible reduced graphene oxide/poly(vinyl alcohol) film with superior microwave absorption properties. *RSC Advances, 5*(108), 88958–88964. https://doi.org/10.1039/C5RA16158D

Wilpiszewska, K., Antosik, A. K., & Zdanowicz, M. (2019). The effect of citric acid on physicochemical properties of hydrophilic carboxymethyl starch-based films. *Journal of Polymers and the Environment, 27*(6), 1379–1387. https://doi.org/10.1007/s10924-019-01436-9

Xiong, X., Tan, Y., Mubango, E., Shi, C., Regenstein, J. M., Yang, Q., Hong, H., & Luo, Y. (2022). Rapid freshness and survival monitoring biosensors of fish: Progress, challenge, and future perspective. *Trends in Food Science & Technology, 129*, 61–73. https://doi.org/10.1016/j.tifs.2022.08.011

Yang, D., Liu, Q., Zeng, X., Chen, X., Li, M., Wu, X., Liu, Y., Zheng, Y., Xiang, J., Wang, C., Weng, W., & Zhang, Y. (2023). Novel pH-responsive indicator films based on bromothymol blue-anchored chitin for shrimp freshness monitoring. *International Journal of Biological Macromolecules, 253*, Article 127052. https://doi.org/10.1016/j.ijbiomac.2023.127052

Yang, X., Zhao, L., Li, L., Ai, M., Wang, K., Hu, Z., Xu, Z., & Liu, X. (2026). Recent advances in extraction and food applications of natural bioactives using deep eutectic solvents. *Food Research International*. , Article 118407. https://doi.org/10.1016/j.foodres.2026.118407

Yin, Y., & Woo, M. W. (2024). Transitioning of petroleum-based plastic food packaging to sustainable bio-based alternatives. *Sustainable Food Technology, 2*(3), 548–566. https://doi.org/10.1039/d4fb00028e

Zhang, Junjun, Zhang, Jianing, Zhang, L., Qin, Z., & Wang, T. (2025). Review of recent advances in intelligent and antibacterial packaging for meat quality and safety. *Foods, 14*(7), 1157. https://doi.org/10.3390/foods14071157

Zhang, T., Guo, Q., Xin, Y., & Liu, Y. (2022). Comprehensive review in moisture retention mechanism of polysaccharides from algae, plants, bacteria and fungus. *Arabian Journal of Chemistry, 15*(10), Article 104163. https://doi.org/10.1016/j.arabjc.2022.104163

Zhao, J., Wang, Y., & Liu, C. (2022). Film transparency and opacity measurements. *Food Analytical Methods, 15*(10), 2840–2846. https://doi.org/10.1007/s12161-022-02343-x

Zouharová, A., Bartáková, K., Bursová, Š., Necidová, L., Haruštiaková, D., Klimešová, M., & Vorlová, L. (2023). Meat and fish packaging and its impact on the shelf life – a review. *Acta Veterinaria Brno, 92*(1), 95–108. https://doi.org/10.2754/avb202392010095